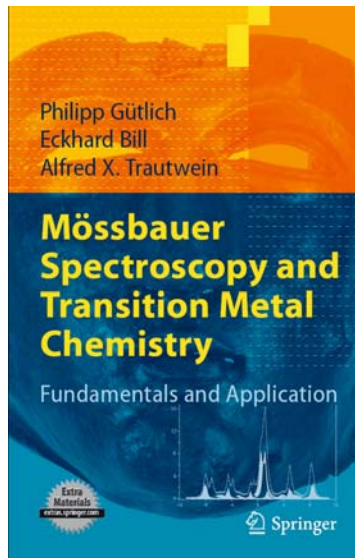


The Mössbauer effect

Resonance fluorescence of nuclear gamma transitions

Some recent Mössbauer literature



Philipp Gütlich

Mössbauer Spectroscopy – Principles and Applications

http://ak-guetlich.chemie.uni-mainz.de/Moessbauer_Lectures_web.pdf

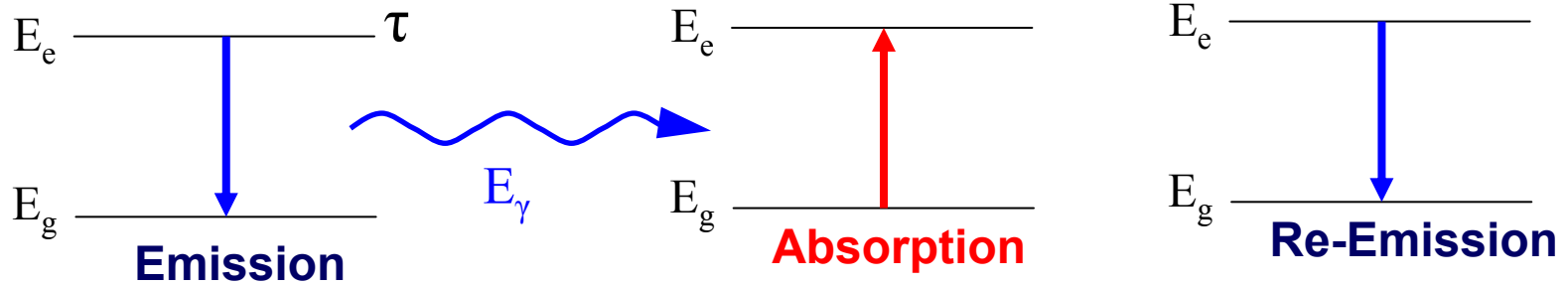
Peter Blaha

Computation and interpretation of Mössbauer parameters from DFT based WIEN2k calculations for extended systems

http://publik.tuwien.ac.at/files/PubDat_195084.pdf

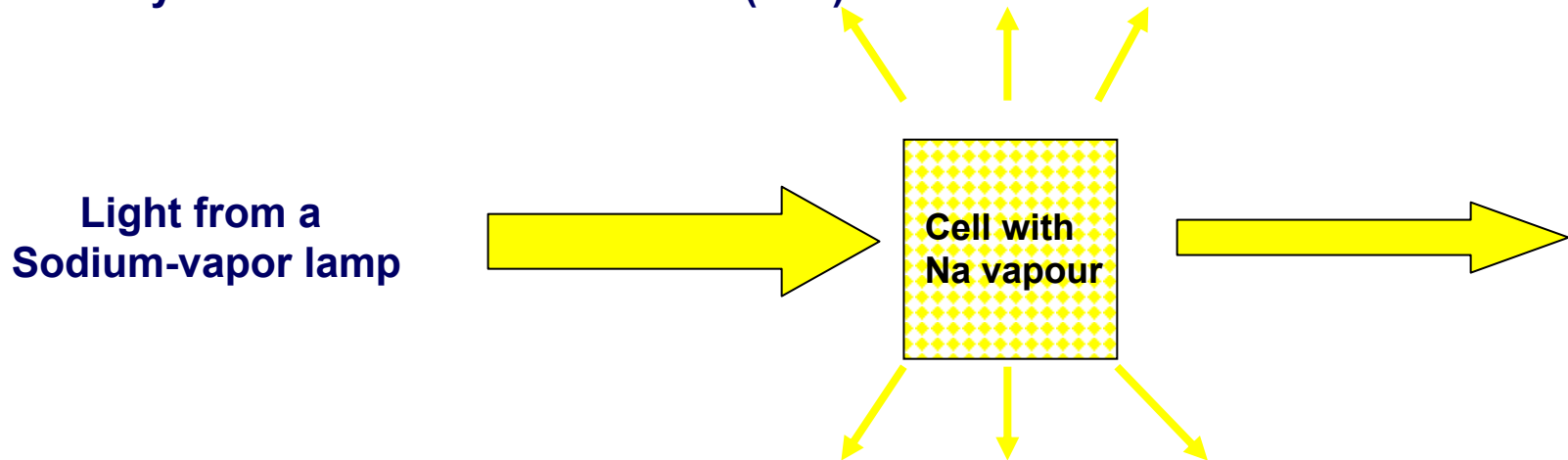
Resonance fluorescence

Absorption and isotropic Re-Emission



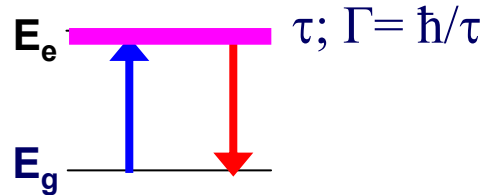
Resonance fluorescence is easily observed with optical transitions (eV)

but usually not with nuclear transitions (keV)



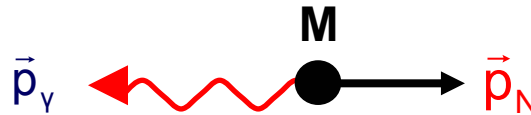
Energy- and Momentum Conservation of Photon-Emission and Absorption

$$E_0 = E_e - E_g$$



$\Gamma = \text{natural line width} = \hbar/\tau$
 Heisenberg uncertainty relation

Momentum conservation



$$|\vec{p}_\gamma| = |\vec{p}_N| = \frac{h\nu}{c} = \frac{E_\gamma}{c} = Mv \quad \longrightarrow \quad v = \frac{E_\gamma}{Mc}$$

Recoil energy $R = \frac{M}{2} v^2 = \frac{E_\gamma^2}{2Mc^2}$ **Emission: $E_\gamma < E_0$**

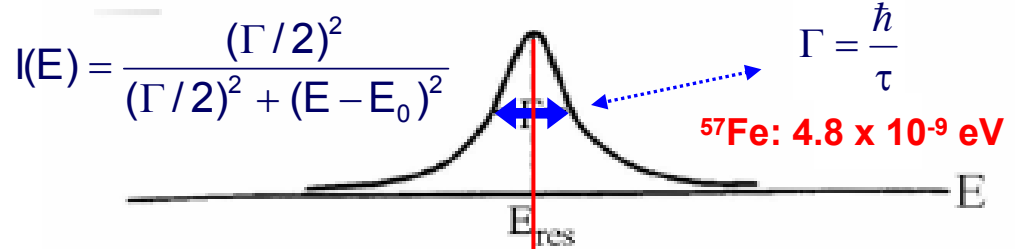
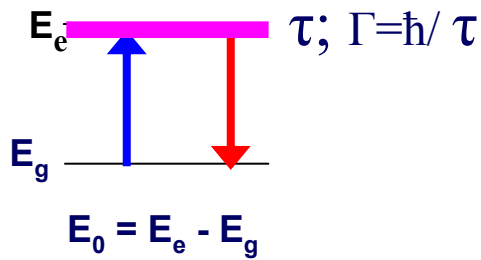
Example ^{57}Fe :



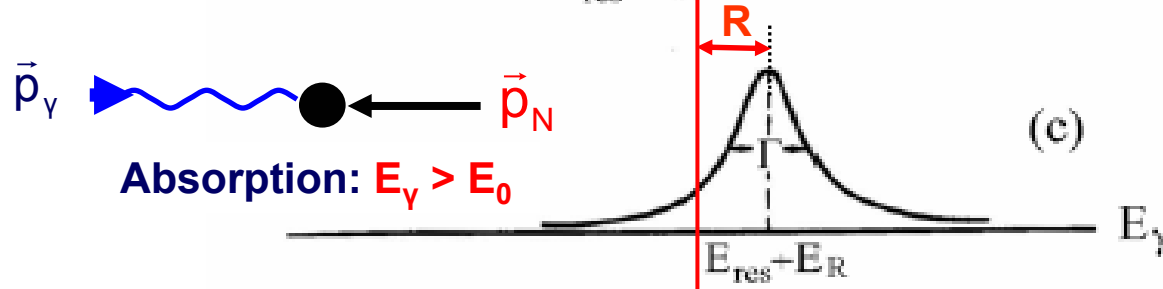
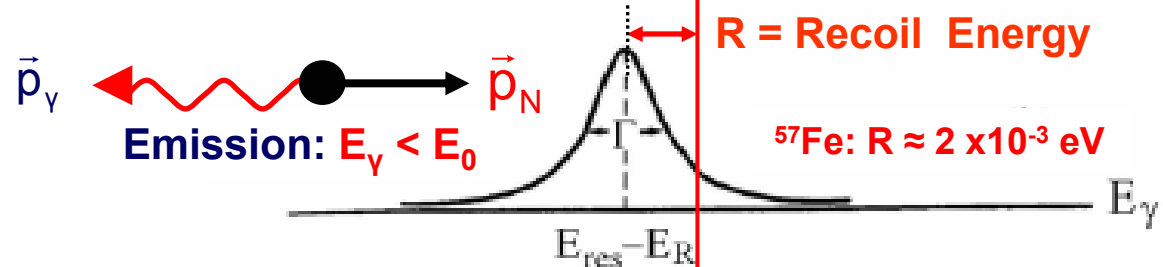
$$R \approx 2 \times 10^{-3} \text{ eV} \sim 4 \times 10^5 \Gamma$$

Energy- and Momentum Conservation of Photon-Emission and Absorption

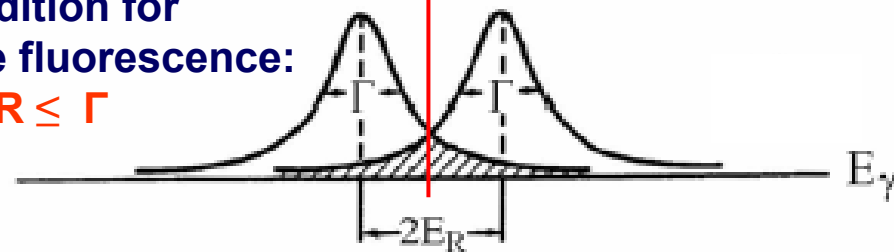
Line width



$$R = \frac{M}{2} v^2 = \frac{E_\gamma^2}{2Mc^2}$$

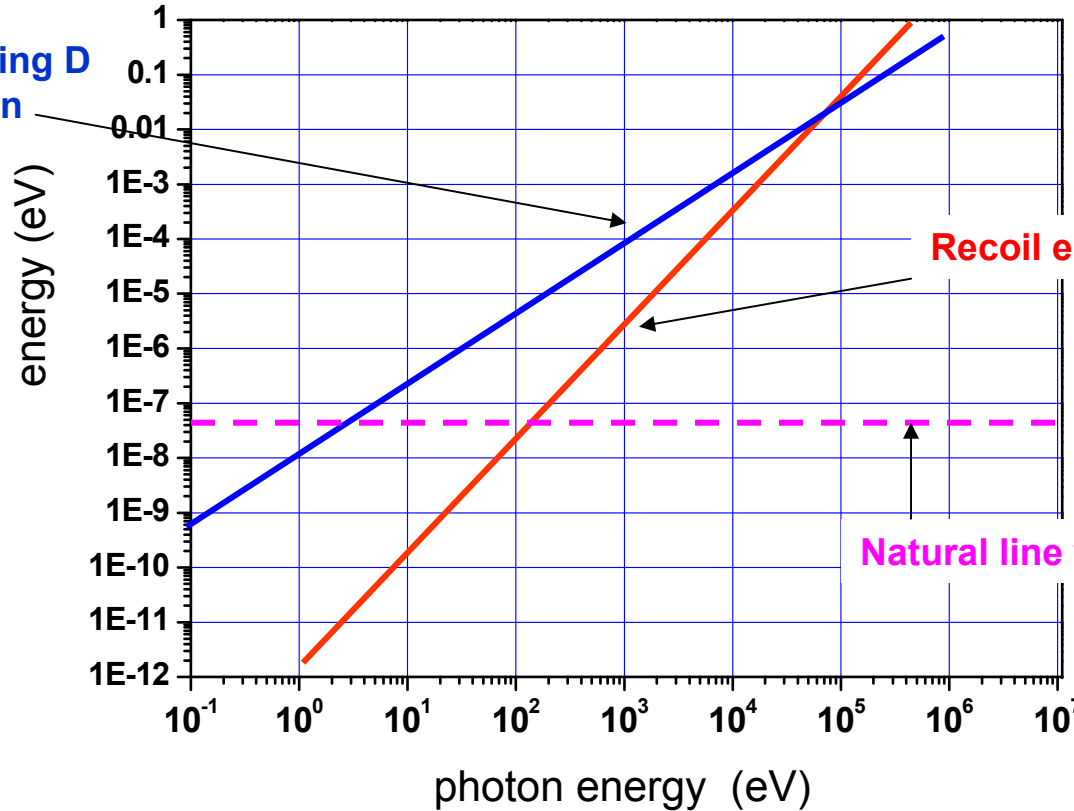


Condition for resonance fluorescence:
 $R \leq \Gamma$



Condition for Resonance Fluorescence

Doppler broadening D
by thermal motion
at $T = 300\text{ K}$



Recoil energy for $M = 100$

Natural line width Γ ($\tau = 10^{-8}\text{ s}$)

$$\Delta E_{\text{Photon}} \times \Gamma \approx \hbar$$

Optical transitions

γ -ray transitions

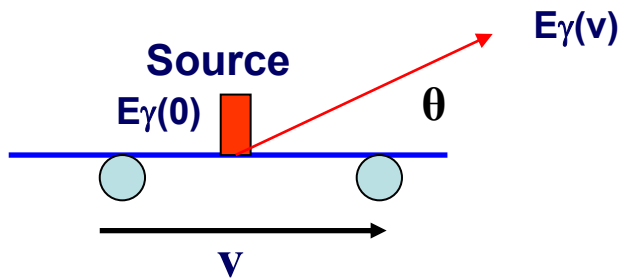
$$\Gamma \geq D, \gg R$$

$$\Gamma \ll R, D$$

Line shift using the Doppler effect

Doppler effect

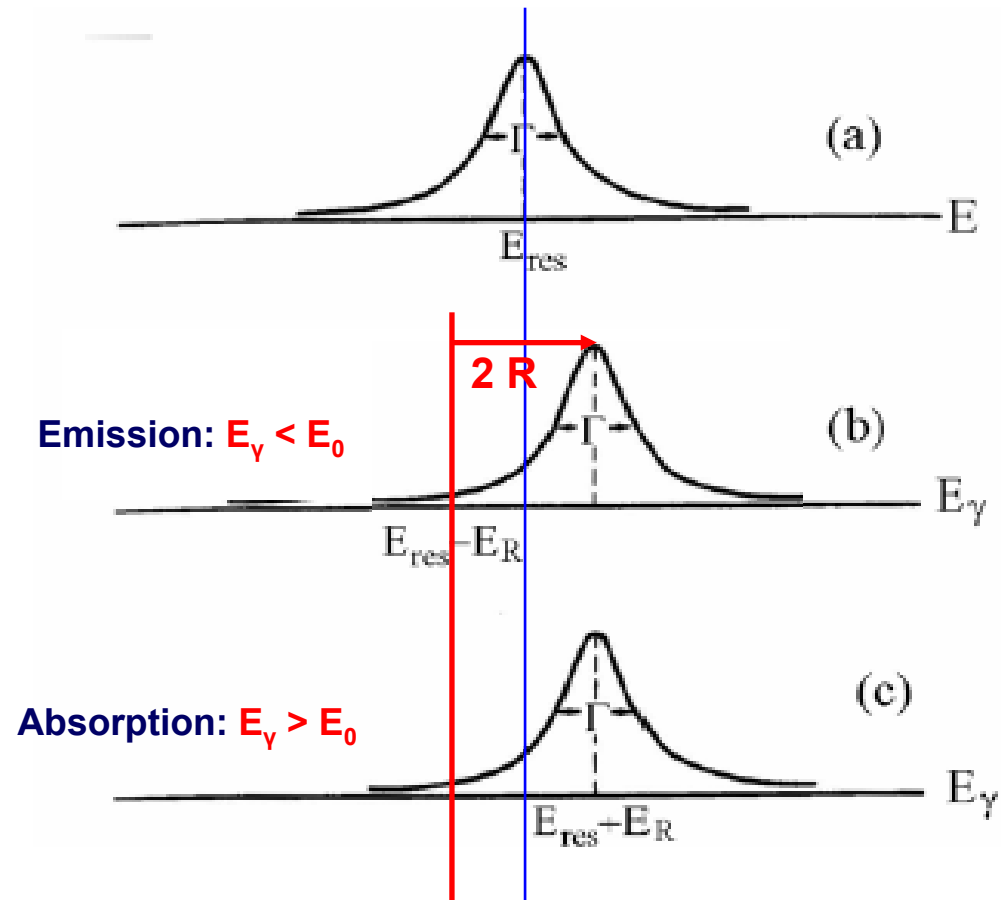
$$E_\gamma(v) = E_\gamma(0) \left(1 + \frac{v}{c} \cos \theta\right)$$



**^{57}Fe : $E_\gamma = 14.4 \text{ keV}$
 $2R \approx 4 \times 10^{-3} \text{ eV}$**

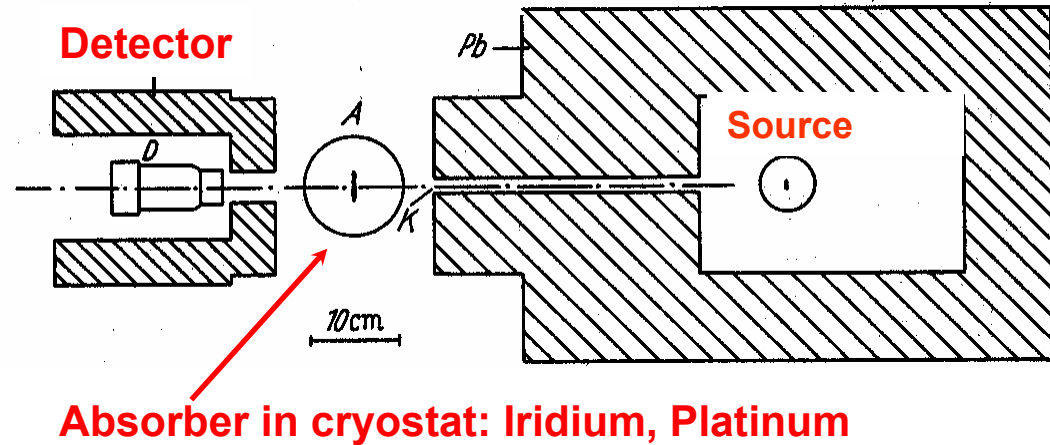
Velocity required to
force resonance by
 moving the source

$$V_{\text{res}} \sim 100 \text{ m/s}$$

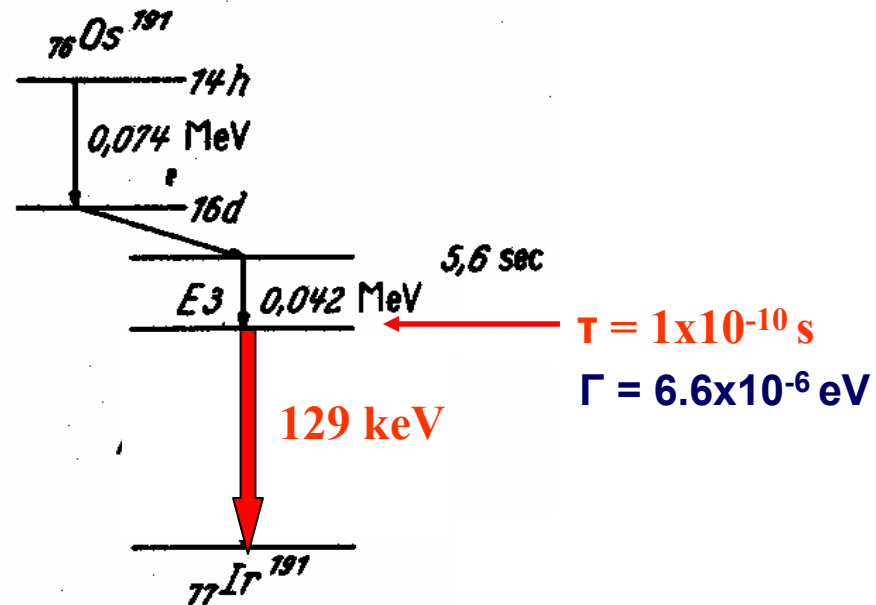


Mössbauers 1. Experiment

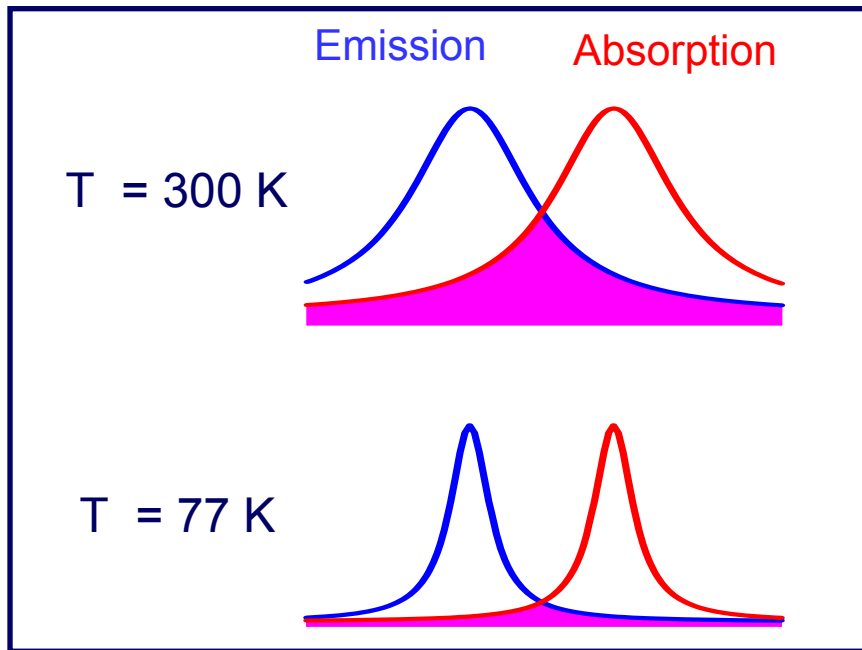
Experimental Set-up



The radioactive source



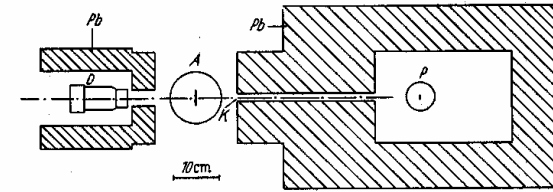
Absorption of the 129 keV-line as a function of absorber temperature



Expectation

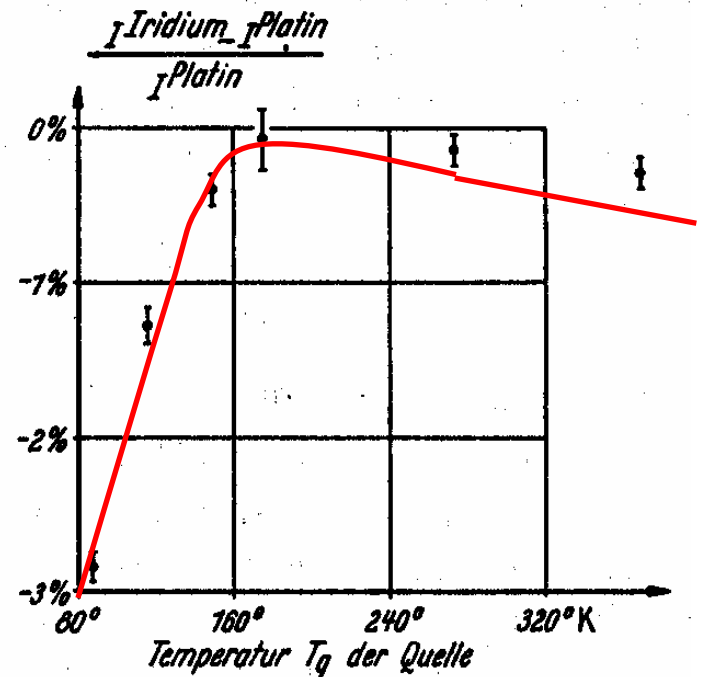
Slower thermal motion leads to narrower lines at lower temperatures

→ Less overlap
Less absorption



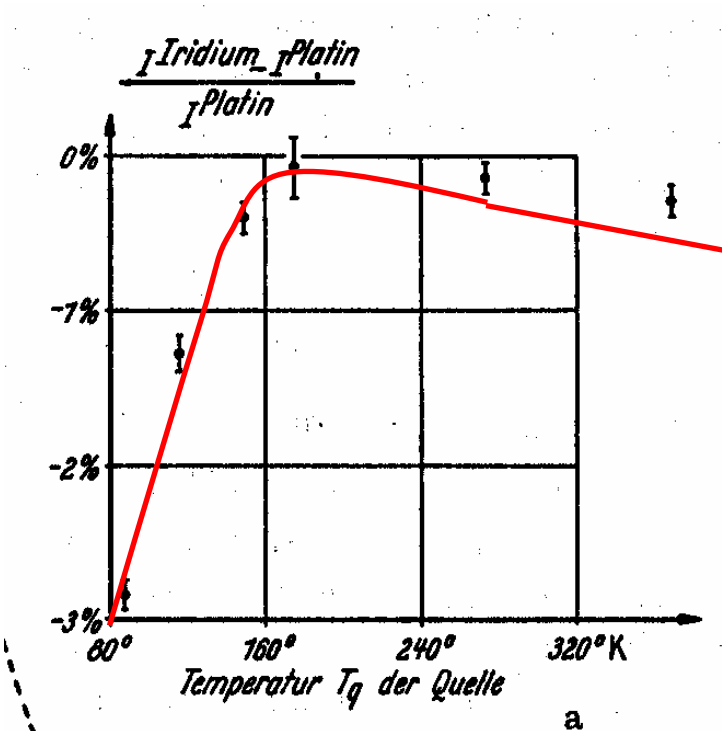
Surprising experimental result:

The absorption increases with decreasing temperature



Result of the 1. Moessbauer experiment

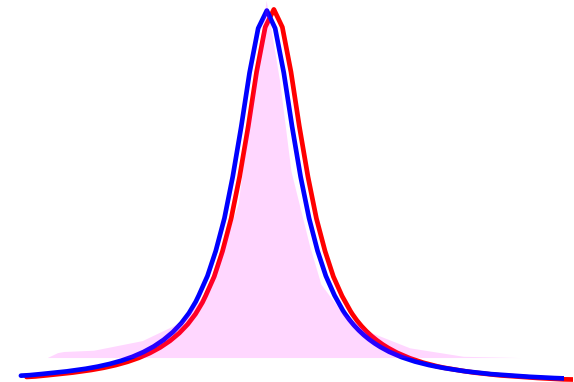
Absorption increases with decreasing temperature



Proposed explanation

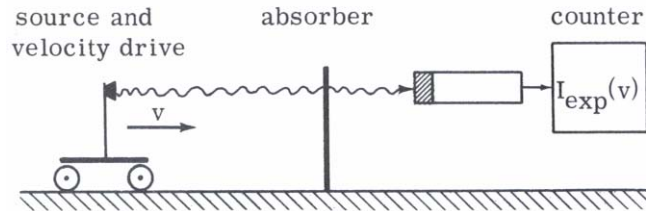
For some fraction of the Ir nuclei the emission- and the absorption line are NOT recoil-shifted relativ to each other:

- Recoil-free emission and absorption
- The recoil-free fraction of γ -quanta (Debye-Waller factor) increases with decreasing temperature

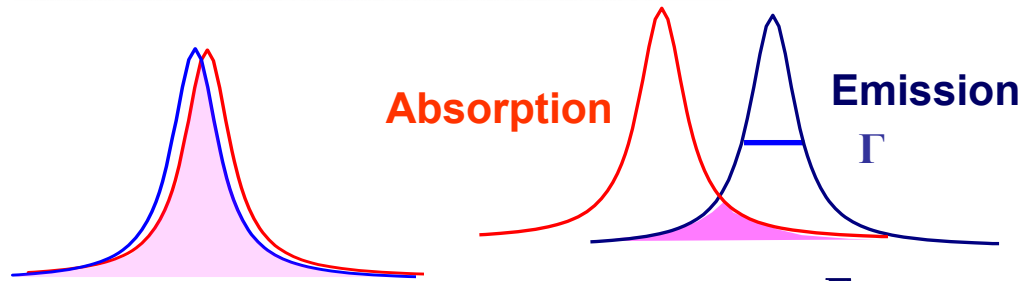


Mössbauers 2. Experiment

Test of the hypothesis of recoil-free emission and absorption



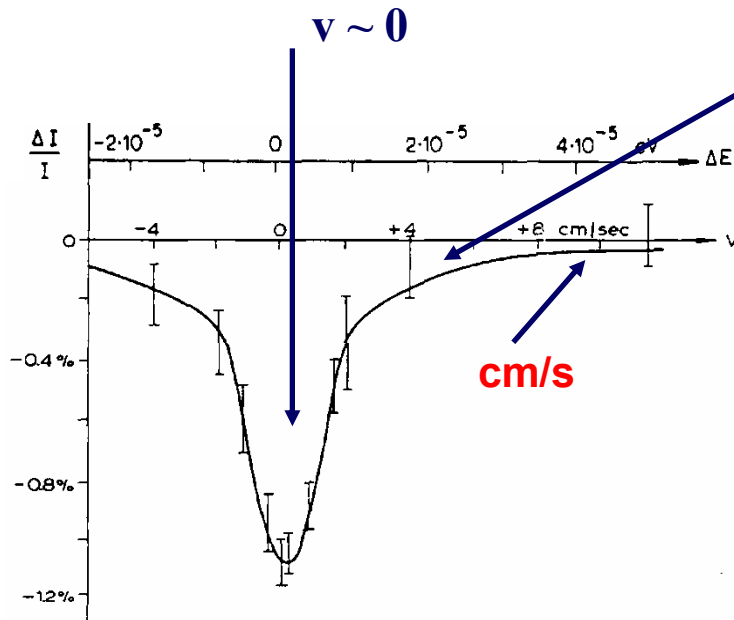
Destruction of the resonance fluorescence by moving the radioactive source



Doppler effect

$$E_\gamma(v) = E_\gamma(0) \left(1 + \frac{v}{c} \cos \theta\right)$$

$$v \approx 2 - 3 \frac{\Gamma \cdot c}{E_\gamma^0}$$



¹⁹¹Ir:

$E_\gamma = 129 \text{ keV}$

$\tau = 1 \times 10^{-10} \text{ s}$

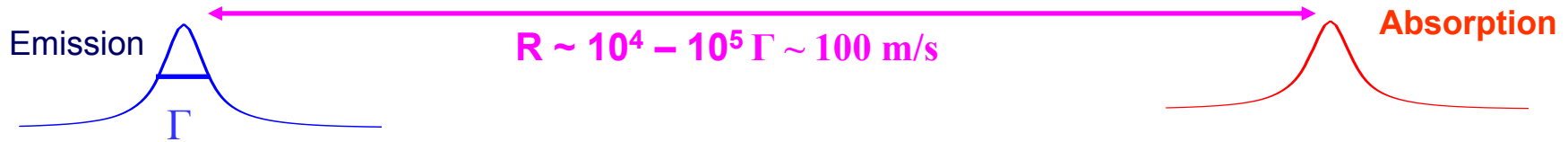
$\Gamma = 6.6 \times 10^{-6} \text{ eV}$

Energy resolution

$\Gamma / E_\gamma \sim 5 \times 10^{-11}$

Recoil-free γ -emission in solids

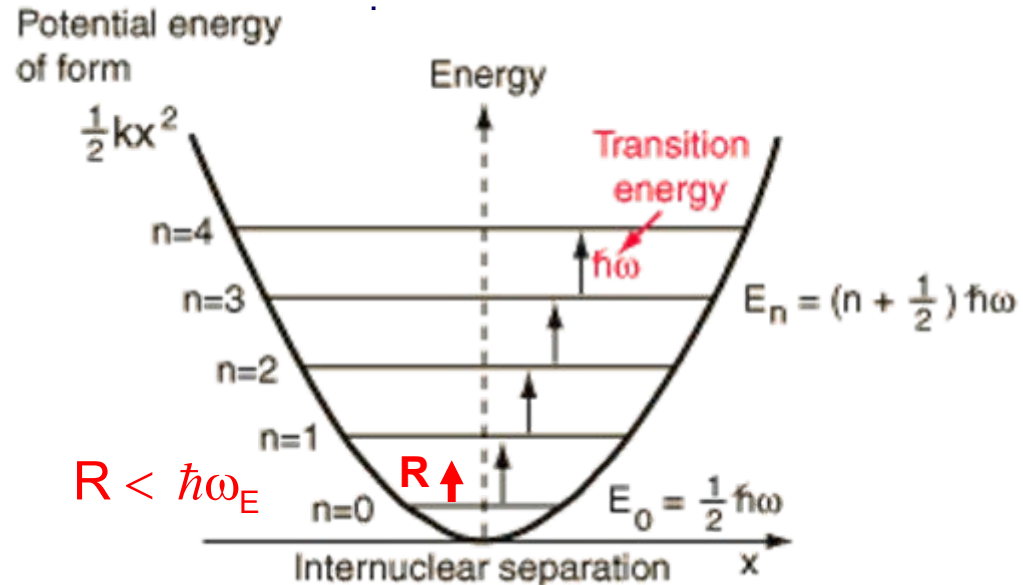
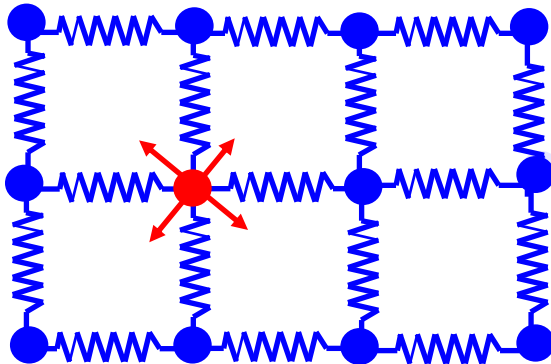
Free nuclei:



The recoil energy can only be dissipated as **kinetic energy** of the emitting/absorbing nuclei.

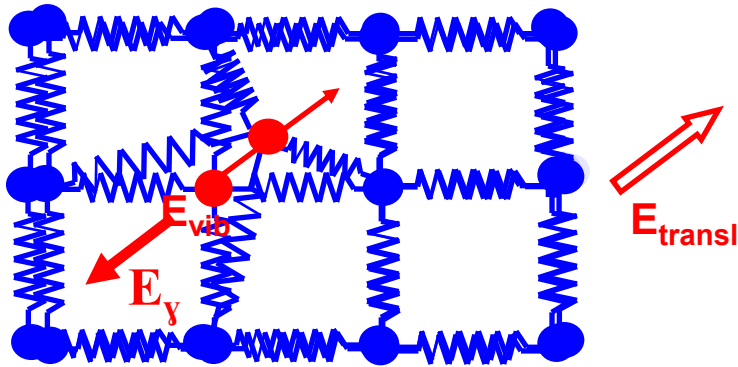
Nuclei in solids

the atoms/nuclei are elastically bound to the lattice and oscillate around their equilibrium position



The energy of these lattice vibrations (phonons) is quantized.

Recoil-less γ -emission in solids - a consequence of quantized lattice vibrations



The recoil energy can be partitioned into a translational part E_{transl} and a vibrational part E_{vib}

$$R = E_{\text{transl}} + E_{\text{vib}}$$

$$E_{\text{vib}} \sim 10^{-3} - 10^{-1} \text{ eV}$$

$$R \sim 10^{-4} - 10^{-1} \text{ eV}$$

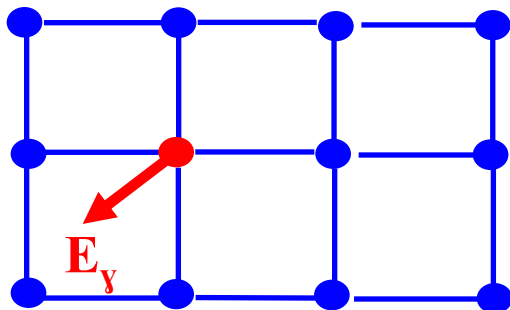
$$\Gamma \sim 10^{-6} \text{ eV}$$

The vibrational energy changes only by discrete amounts $0, \pm \hbar\omega, \pm 2\hbar\omega$:
phonon transitions

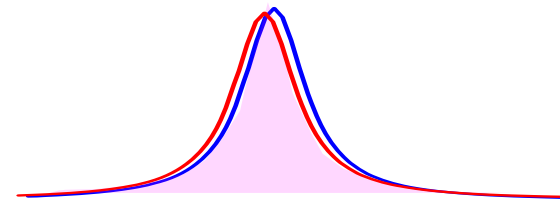
There is a finite probability that the gamma-emission does not **change the quantum state of the lattice**.

In the case of a **such zero-phonon transition, the nucleus is bound into a rigid lattice**. The entire crystal ($\sum_n M_n$) takes the recoil, the loss of energy of the emission- (and absorption-) γ -line is practically zero.

$$R = \frac{E_\gamma^2}{2 \sum_n M_n c^2}$$



Recoil-free emission and absorption



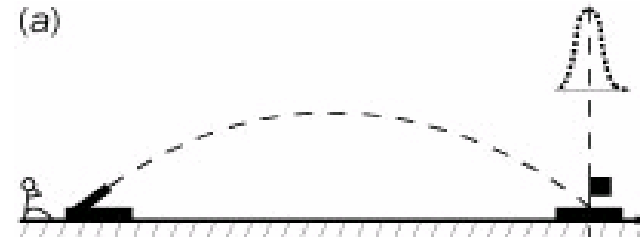
Mössbauer's analogy

Translation from Mössbauer's thesis

This situation (is)...like a person throwing a stone from a boat.

The majority of the energy is submitted to the stone, but a small amount goes into the kinetic energy of the recoiling boat. During the summer time, the boat will simply pick up this recoil energy.

If, however, the person throws the stone during winter time, with the boat frozen into the lake, then practically all energy is going into the stone thrown and only a negligible amount is submitted to the boat. The entire lake will, thus, take up the recoil and this procedure occurs as recoilless process.



Cannon on firm ground firing at target. The bell-shaped curve represents the distribution of the shells around the target.



Cannon is now on the lake. Recoil makes the shots fall short of target by the recoil distance, R .



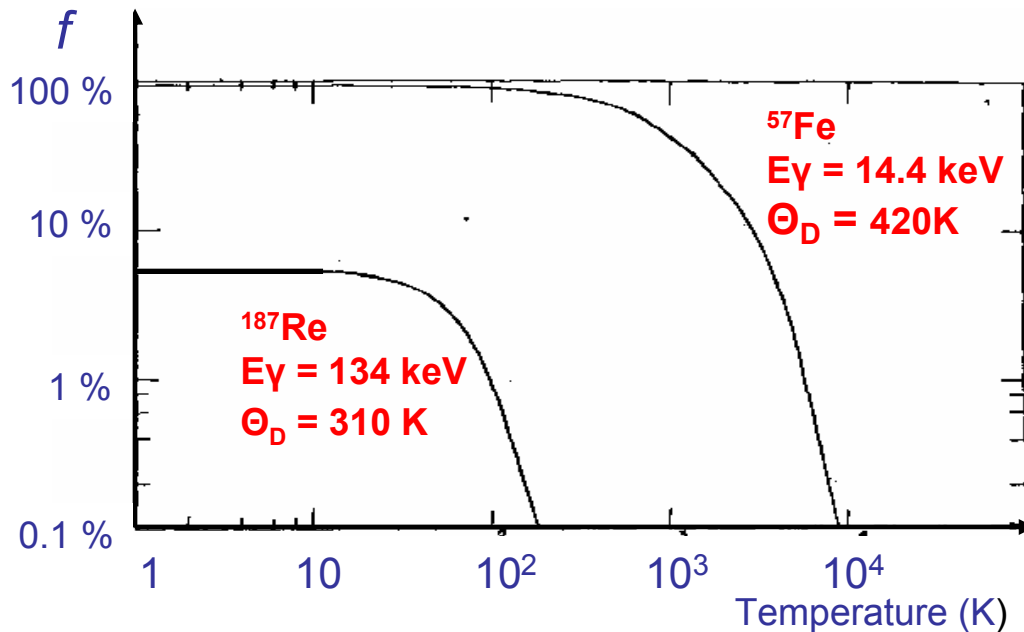
The cannon is floating on a choppy lake. Recoil occurs and the shells fall short of the same recoil distance R . Now the motion of the lake causes the distribution of the shells to broaden. This effect is the same as thermal broadening in atoms.

Debye-Waller-Factor – recoil-free fraction

$$f = \exp \left\{ - \frac{6E_R}{k_B \Theta_D} \left[\frac{1}{4} + \left(\frac{T}{\Theta_D} \right)^2 \int_0^{\Theta_D/T} \frac{z}{e^z - 1} dz \right] \right\}$$

Θ_D = Debye temperature:

$$k_B \Theta_D = \hbar \omega_D$$



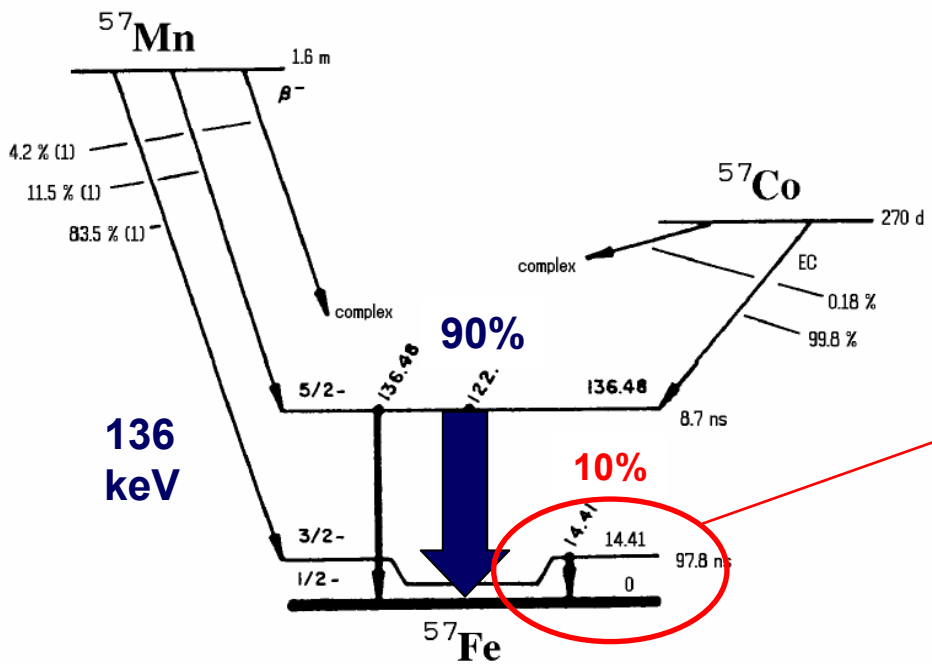
The recoil-free fraction *increases*

- a) with decreasing recoil energy E_R
- b) with decreasing temperature T
- c) with increasing Debye-temperature (bondstrength)

Mössbauer Elements

K	Ca	Sc	Ti	V	Cr	Mn	Fe	Co	Ni	Cu	Zn	Ga	Ge	As	Se	Br	Kr	
Rb	Sr	Y	Zr	Nb	Mo	Tc	Ru	Rh	Pd	Ag	Cd	In	Sn	Sb	Te	I	Xe	
Cs	Ba	La	Hf	Ta	W	Re	Os	Ir	Pt	Au	Hg	Tl	Pb	Bi	Po	At	Rn	
Fr	Ra	Ac																
			Ce	Pr	Nd	Pm	Sm	Eu	Gd	Tb	Dy	Ho	Er	Tm	Yb	Lu		
			Th	Pa	U	Np	Pu	Am	Cm	Bk	Cf	Es	Fm	Md	No	Lw		

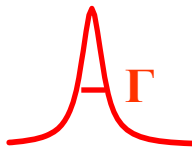
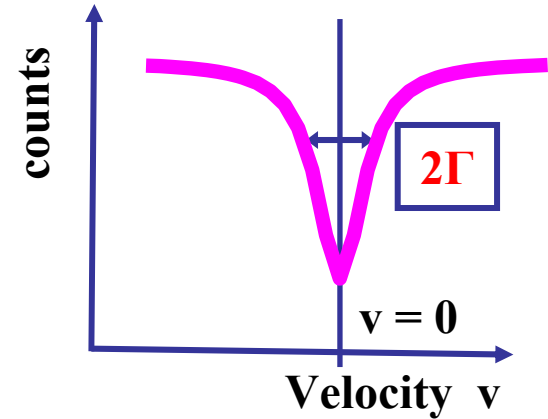
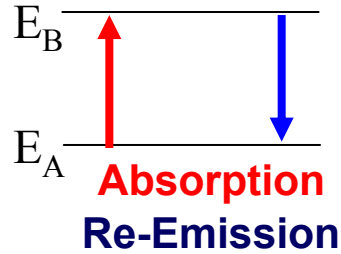
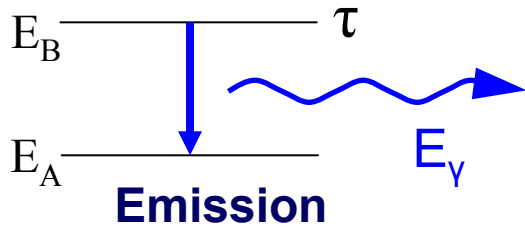
^{57}Fe – the most popular Mössbauer isotope



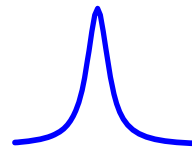
Energy resolution:
 $\Gamma/E_\gamma = 3.3 \cdot 10^{-13}$!!!

Mössbauer Geometries

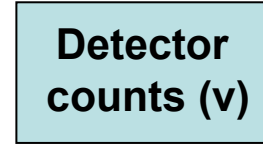
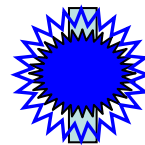
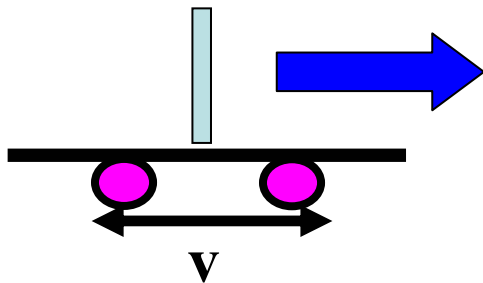
Transmission Geometry



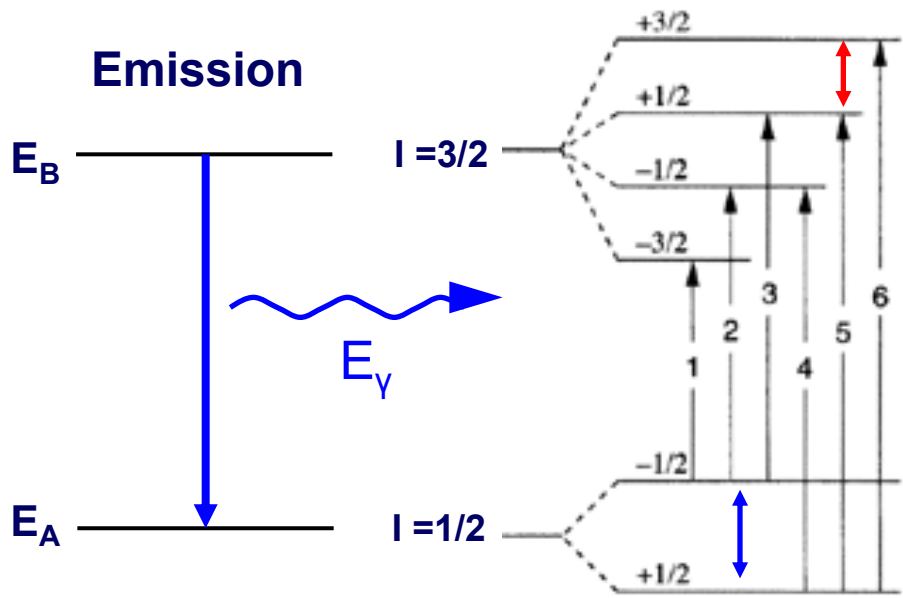
Source (CoRh)



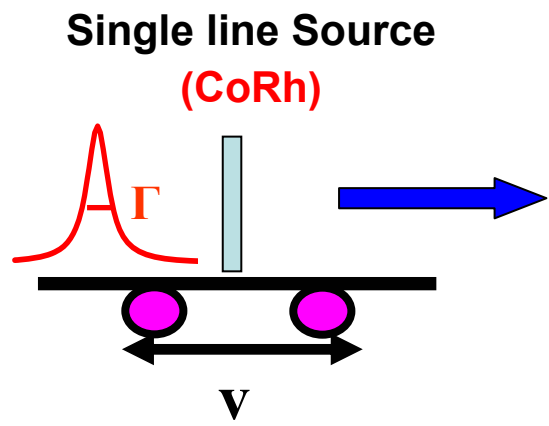
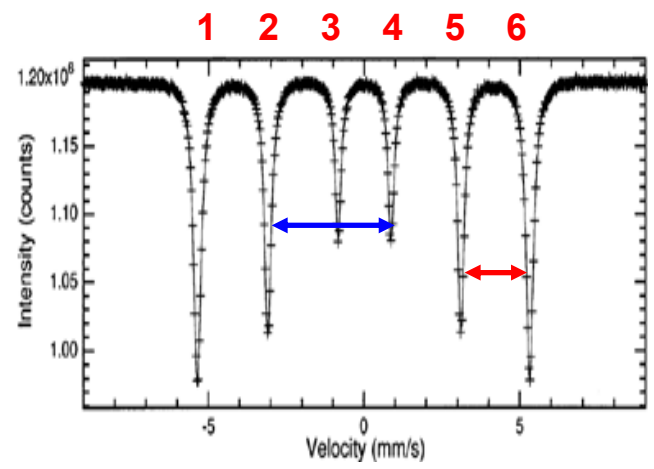
Absorber



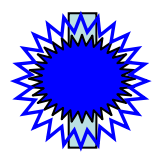
Magnetically split absorber (bcc Fe) in Transmission Geometry



Selection rule $\Delta I = \pm 1, \Delta m_I = 0, \pm 1$ excludes $1/2 \rightarrow -3/2$ and $-1/2 \rightarrow 3/2$ transitions



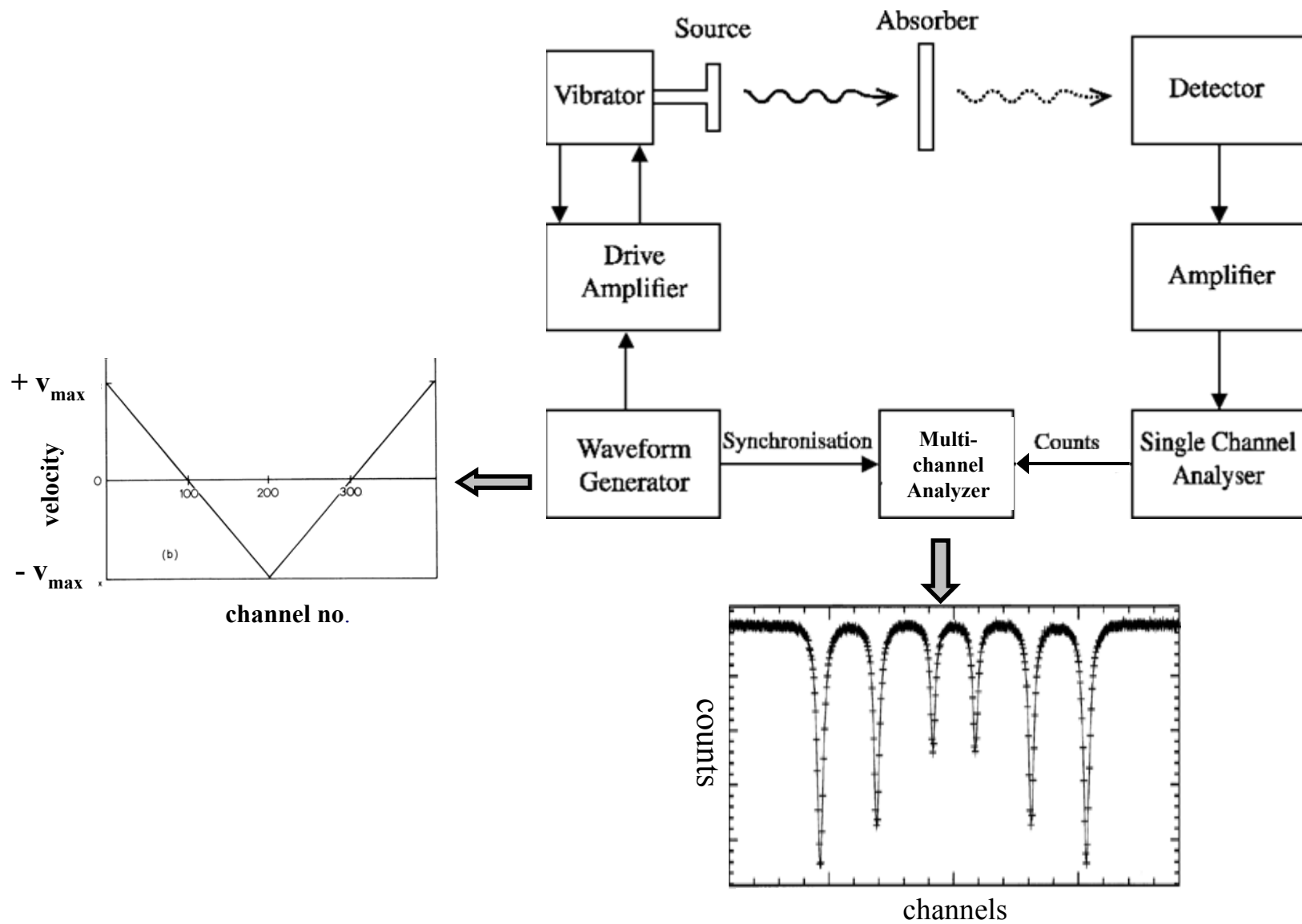
Absorber



Detector counts (v)



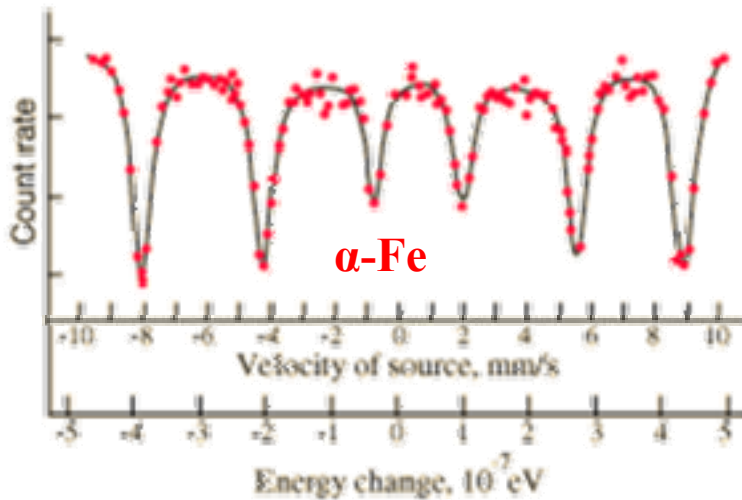
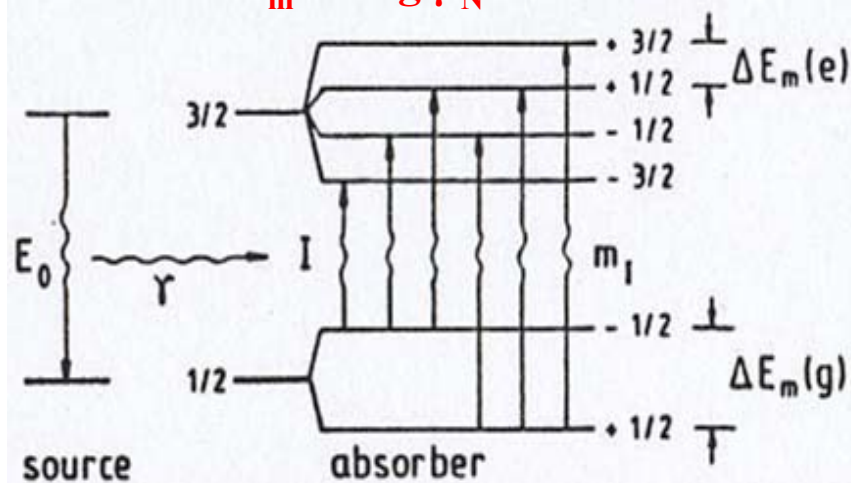
Mössbauer spectrometer schematic



Mössbauer spectra and hyperfine interactions

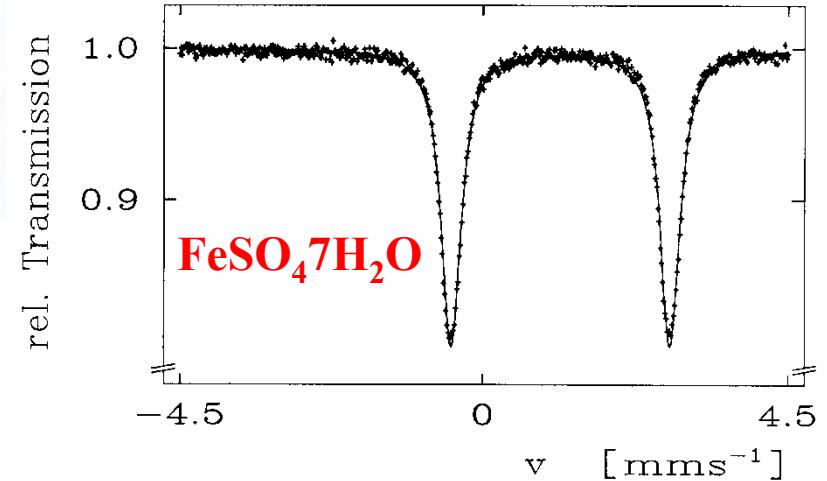
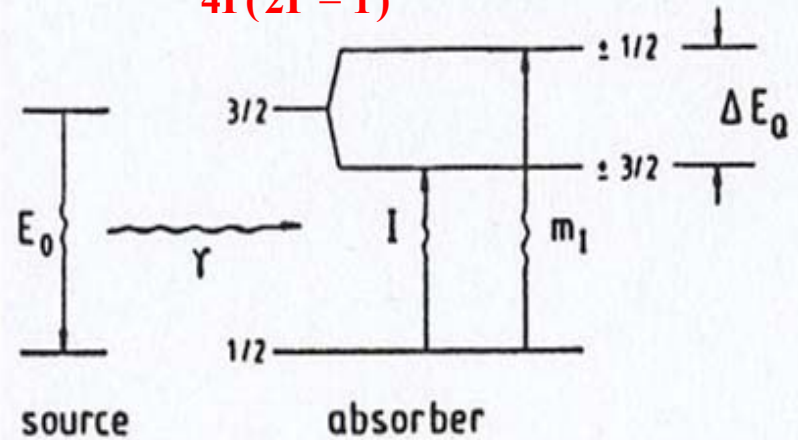
Magnetic interaction

$$E_m = m g \mu_N B_z$$

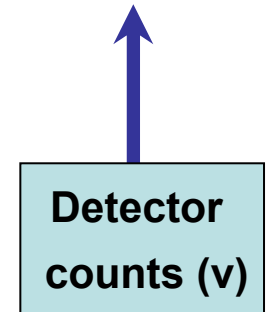
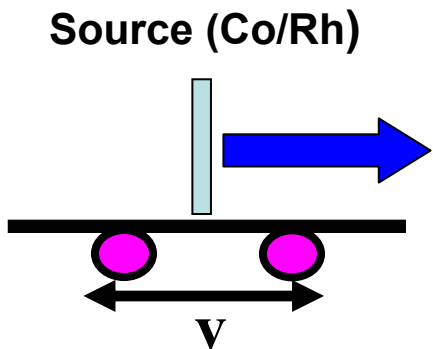
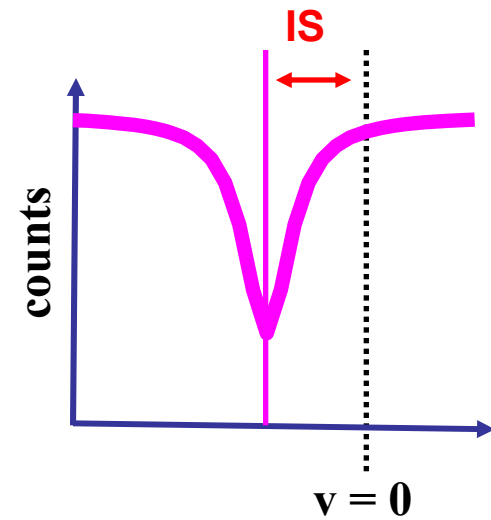
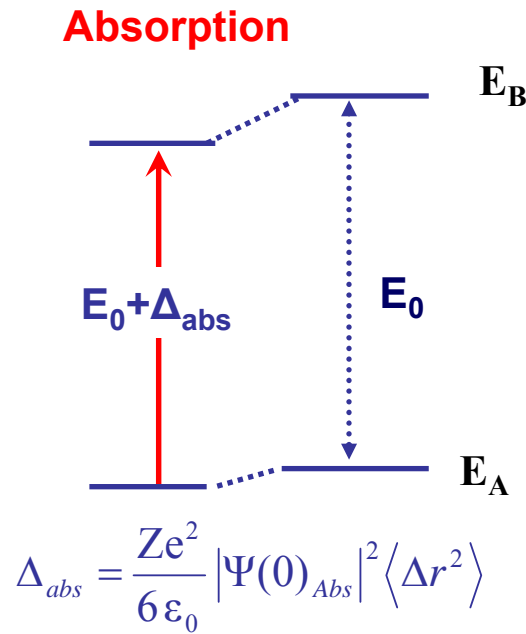
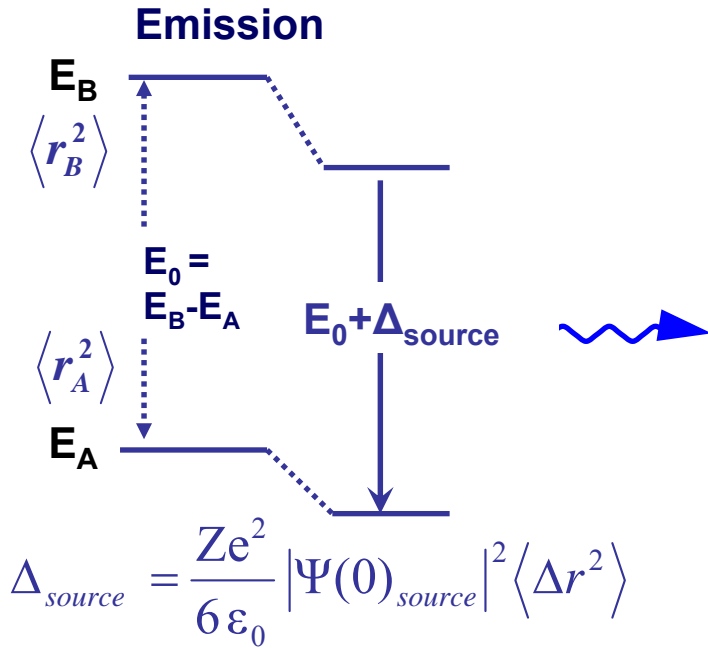


Quadrupole interaction

$$E_m^Q = \frac{eQV_{zz}}{4I(2I-1)} \{3m^2 - I(I+1)\}$$



Isomer Shift in Mössbauer spectra



$$IS = \frac{Ze^2}{6\epsilon_0} \left\langle \left| \Psi_{source}(0) \right|^2 - \left| \Psi_{absorber}(0) \right|^2 \right\rangle (R_A^2 - R_B^2)$$

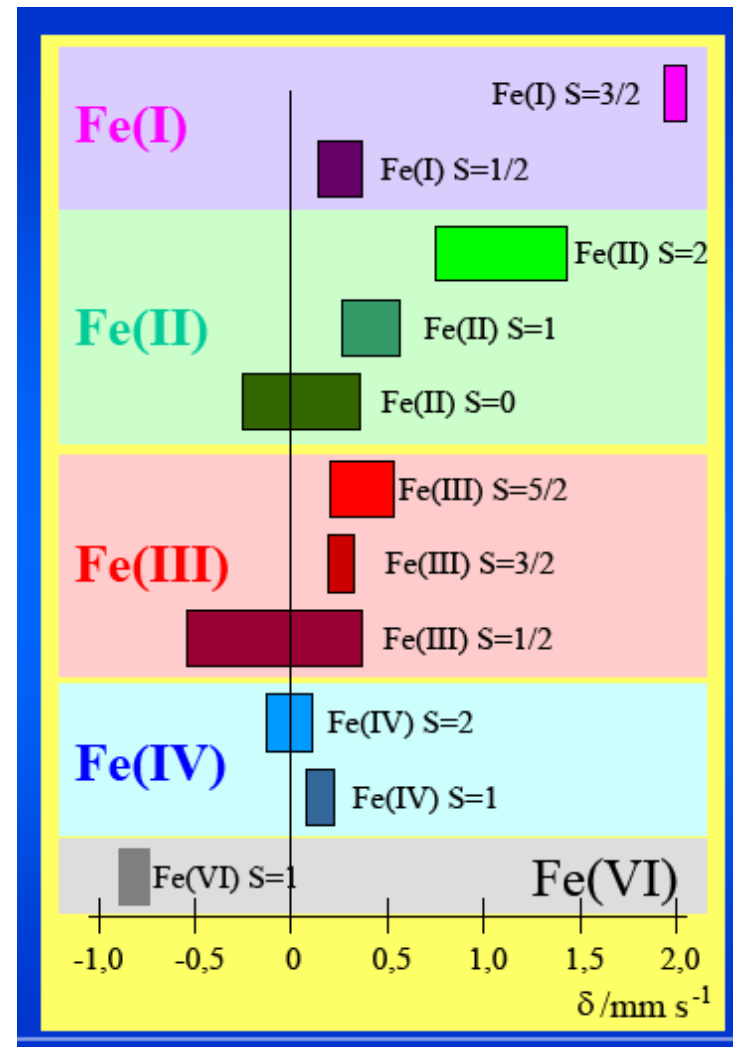
Isomer Shifts of Iron Compounds

$$IS = \frac{Ze^2}{6\epsilon_0} \left\langle \left| \Psi_A(0) \right|^2 - \left| \Psi_S(0) \right|^2 \right\rangle (R_e^2 - R_g^2)$$

For ^{57}Fe : $(R_e^2 - R_g^2) < 0$

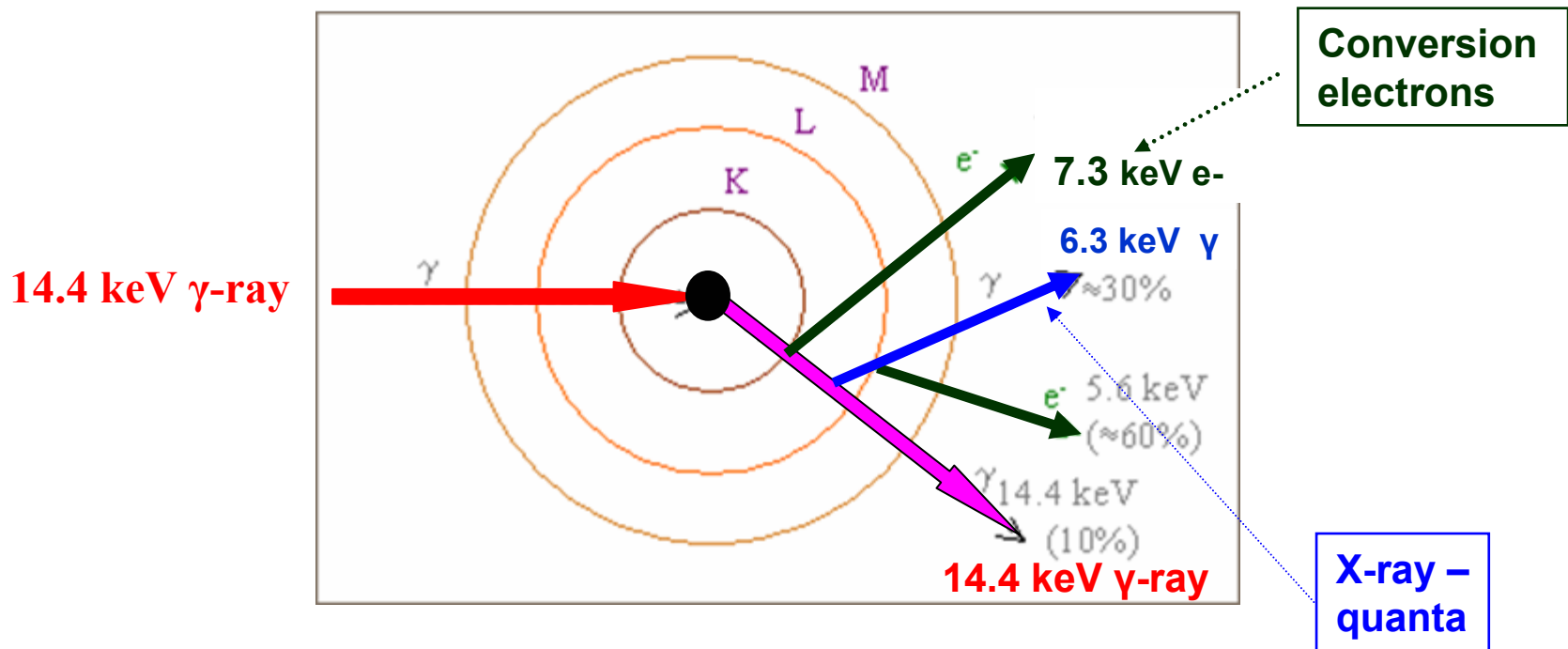
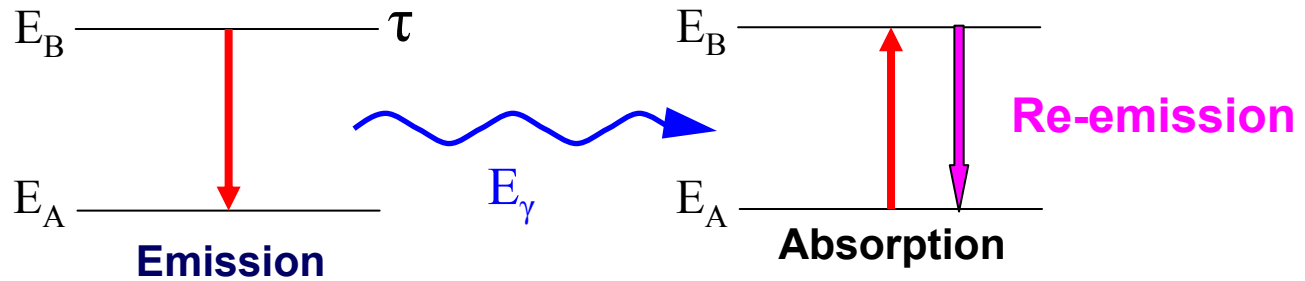
With the same source $(|\Psi(0)|_S)^2 = \text{const.}$

$$\text{Shift } \Delta = C |\Psi(0)|_A^2 (R_e^2 - R_g^2)$$

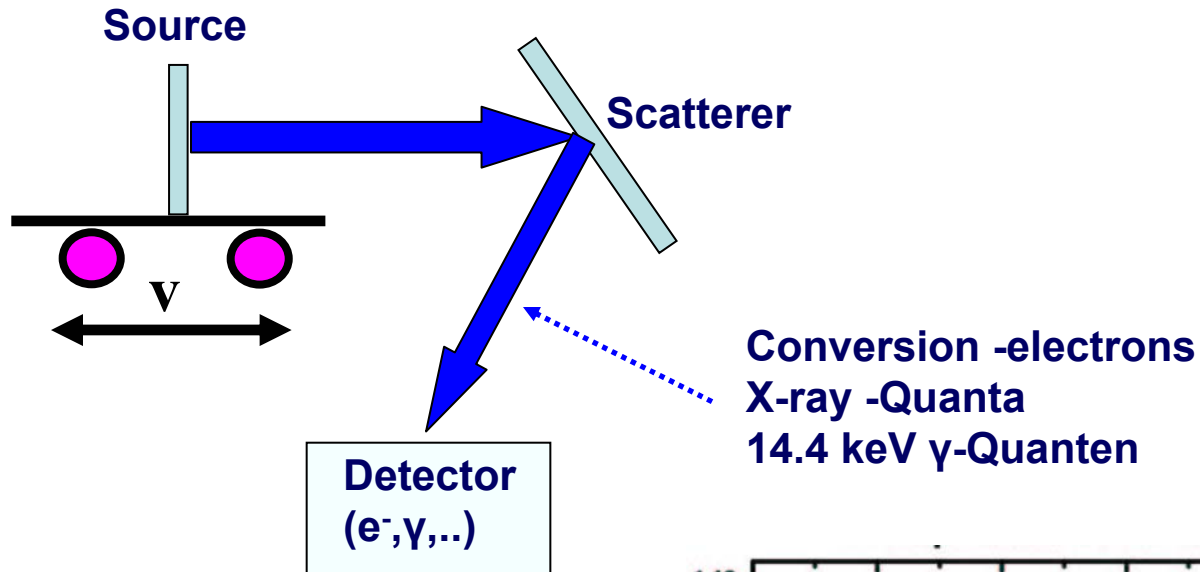


← Increasing $|\Psi(0)|_A^2$

Re-emission processes with ^{57}Fe as example



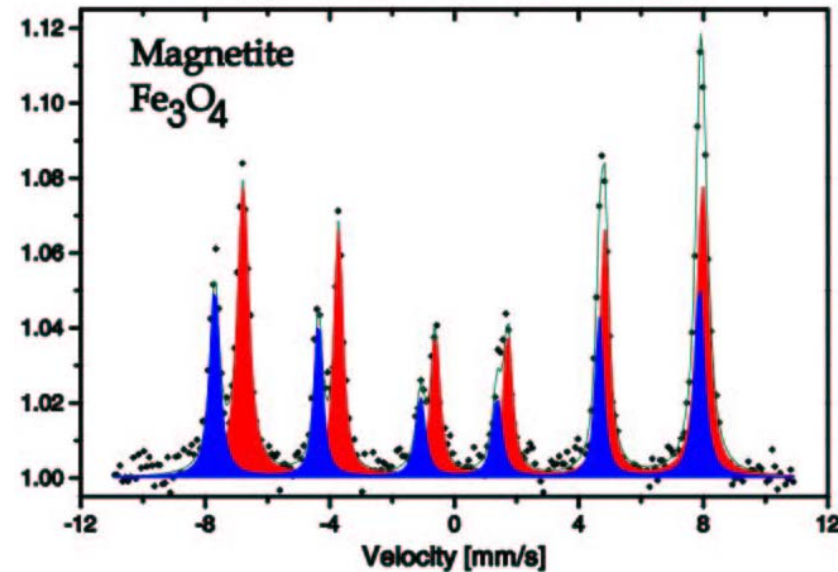
Backscattering Geometry



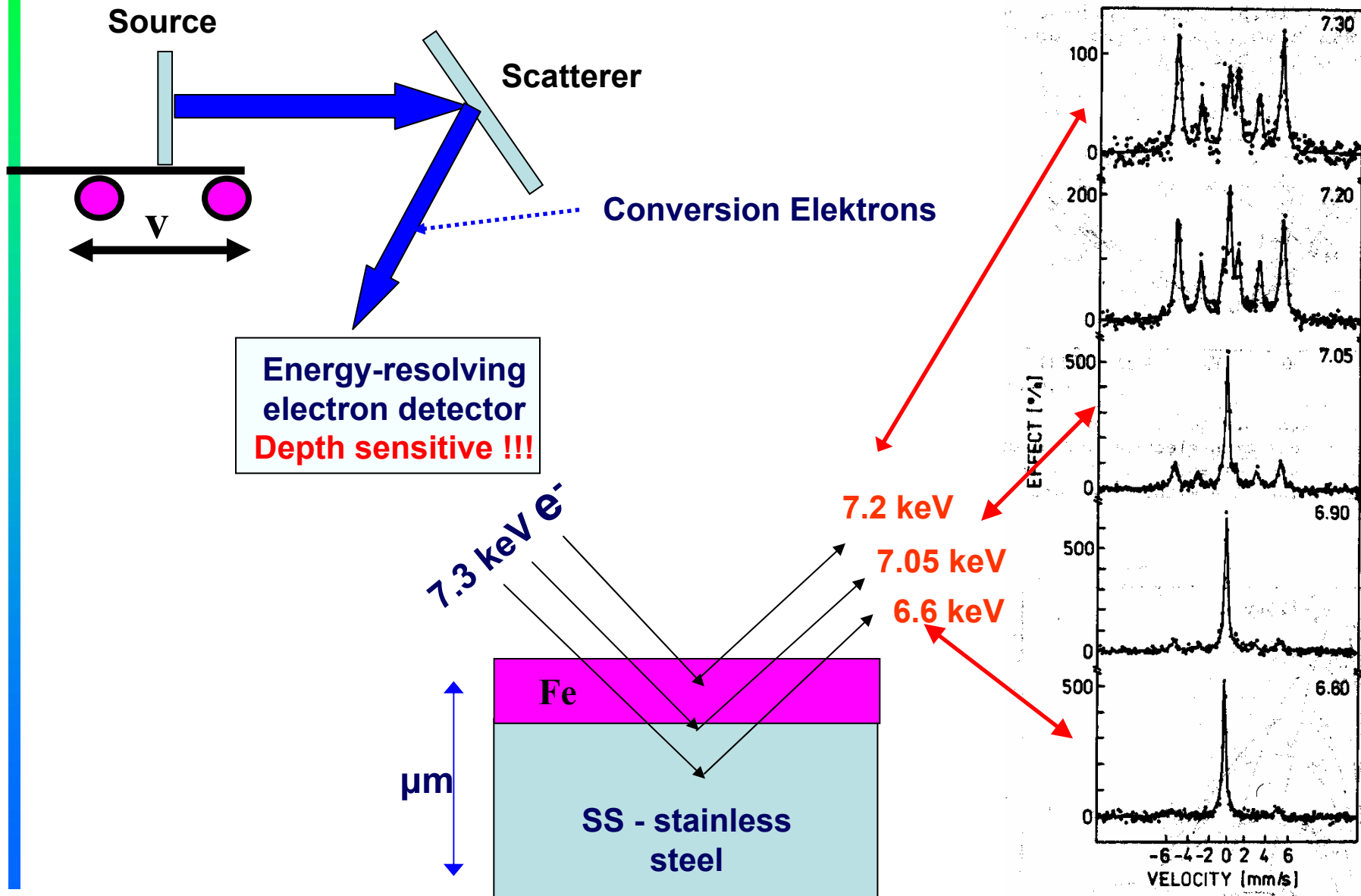
CEMS

Conversion Electron Moessbauer Spectroscopy

CEMS Spektrum von Magnetite (Fe₃O₄)

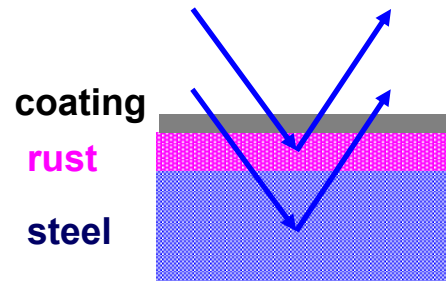
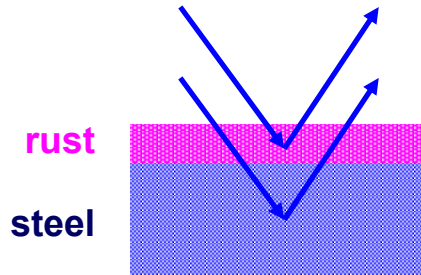
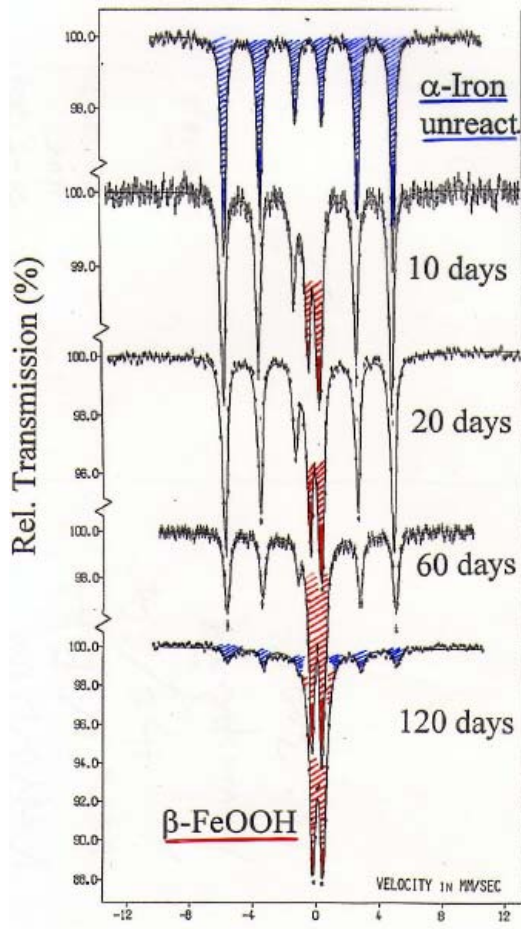


DCEMS : Differential Conversion Electron Mössbauer Spectroscopy

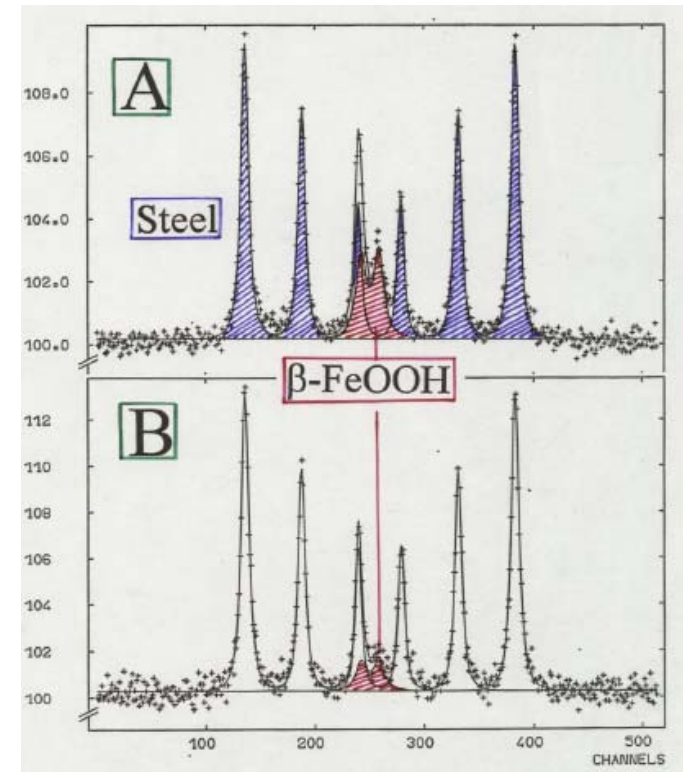


Industrial applications: Mössbauer study of corrosion

α -Fe foil in H_2O/SO_2 atmosphere



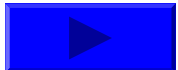
CEMS study of corrosion inhibition



Applications of Mössbauer Spectroscopy

HFI Parameter	Nuclear Physics	Solid State Physics	Chemistry
Isomerie-Shift	Nuclear Radii	Electron densities Electronic structure	Valencies
Magnetic HFI $\omega_L \propto (\mu \cdot B_{hf})$	Nuclear Moments	Magnetic Structures Relaxation phenomena	Properties of magnetic Ions Catalysis e.g. Fischer-Tropsch synthesis
Electric QWW $\omega_Q \propto (Q \cdot V_{zz})$ η		Charge distributions (strength, symmetry)	Ligand Symmetries Phase Identification
Debye-Waller Factor		Phonon spectra	Anisotropic Ligands

SR



The Athena MIMOS II Mössbauer Spectrometer Investigation

G. Klingelhöfer¹, R.V. Morris², B. Bernhardt¹, D. Rodionov^{1,3}, P. A. de Souza Jr.^{1,4},
S. W. Squyres⁵, J. Foh¹, E. Kankeleit⁶, U. Bonnes⁶, R. Gellert¹, Ch. Schröder¹, S. Linkin³,
E. Evlanov³, B. Zubkov³, and O. Prilutski³

¹Institut Inorg. & Analytical Chemistry, Johannes Gutenberg-University, 55099 Mainz, Germany

²NASA Johnson Space Center, Houston, TX 77058, USA

³Space Research Institut IKI, Moscow, Russia

⁴Pelletizing Department, Companhia Vale do Rio Doce, Vitoria, ES, Brazil

⁵Cornell University, Ithaca, NY 14853, USA

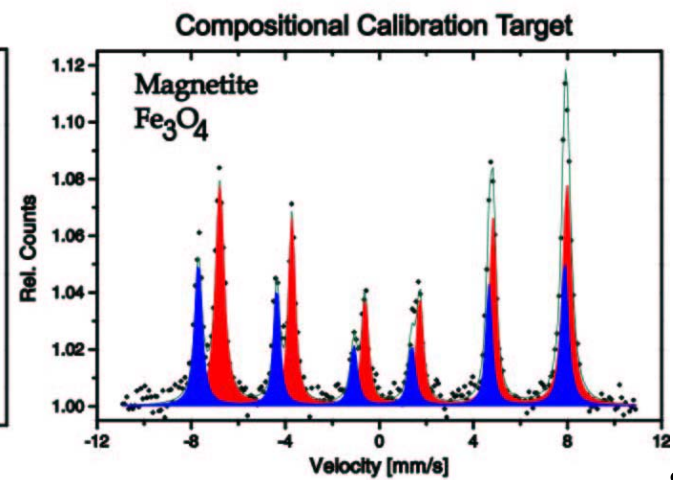
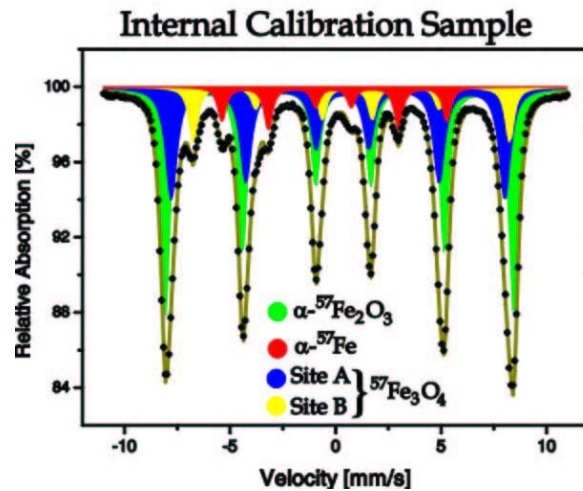
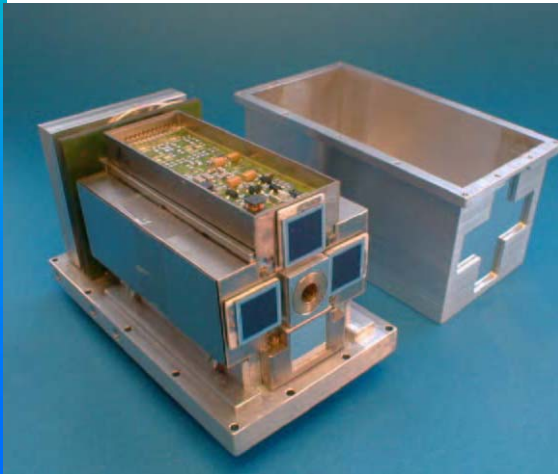
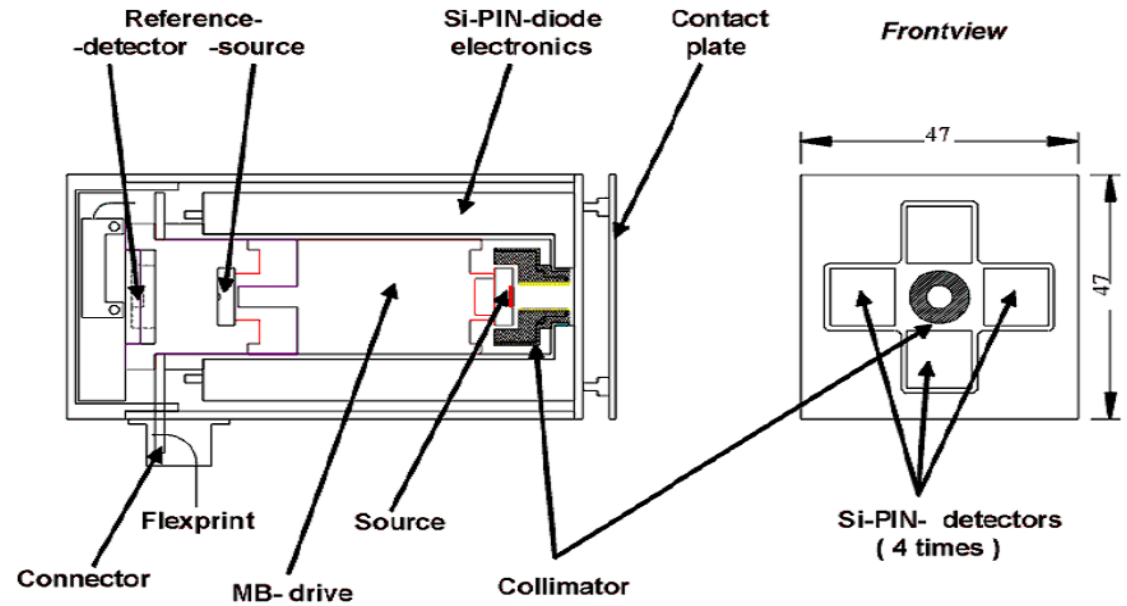
⁶Nuclear Physics Institut, Darmstadt University of Technology, 64289 Darmstadt, Germany

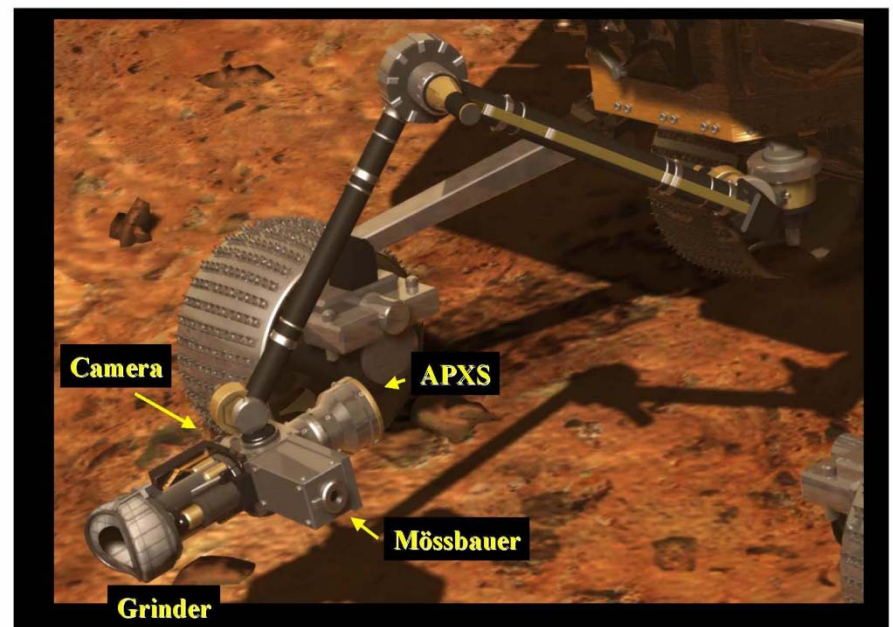
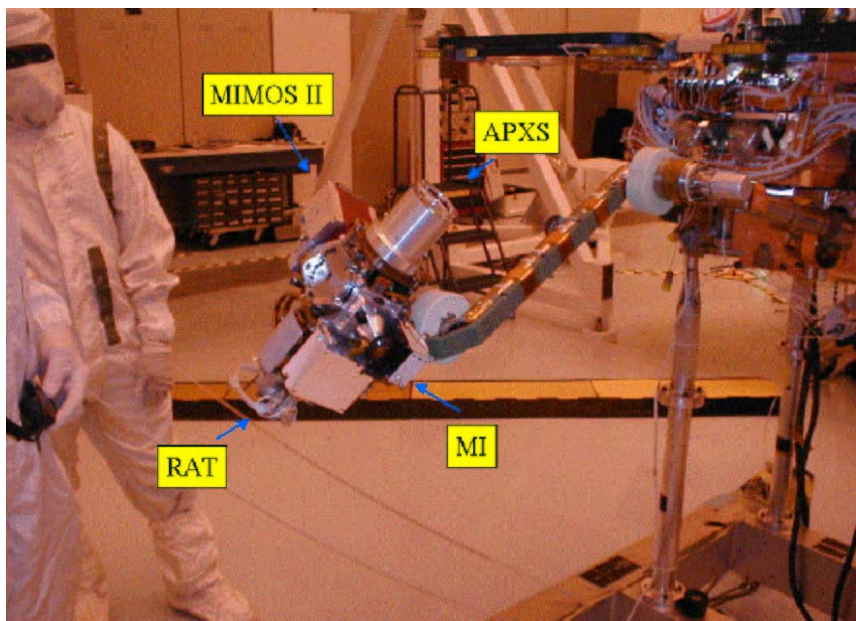
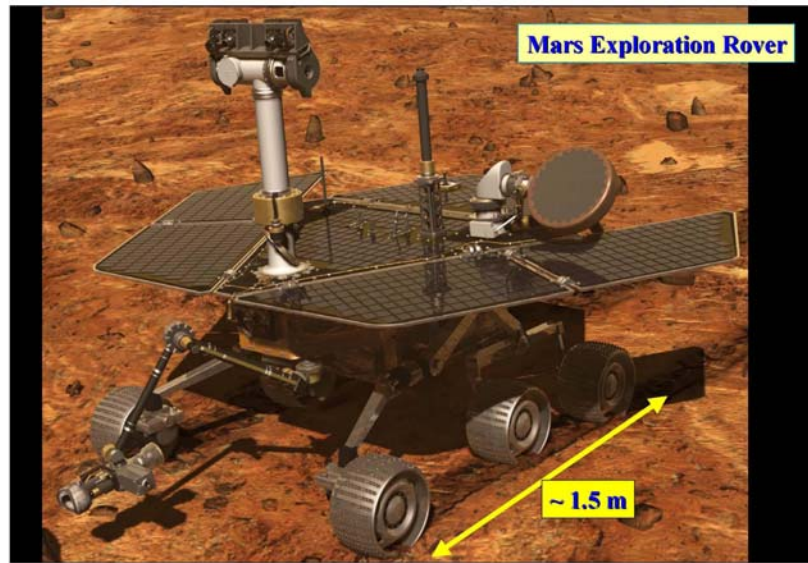
Athena = Scientific Program of Rover Mars Expedition - started in 2003

MIMOS = Miniaturized Mössbauer Spectrometer

Backscattering geometry: does not require sample preparation !!!

DESIGN of MIMOS II



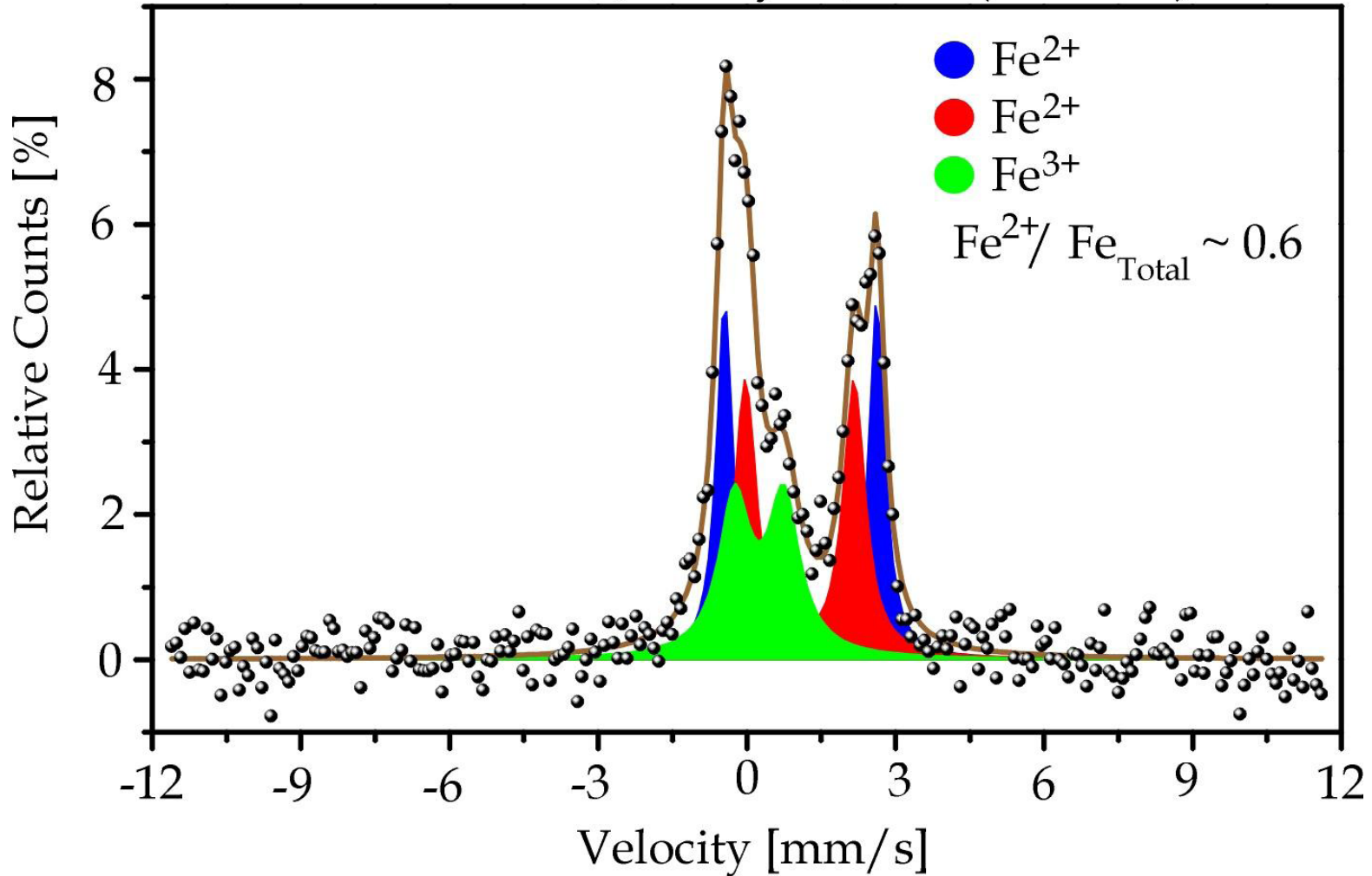


The scientific measurement objectives of the MIMOS II on Mars investigation

are to obtain **quantitative mineralogical analysis of Fe-bearing materials** (rock, soil, and dust) by

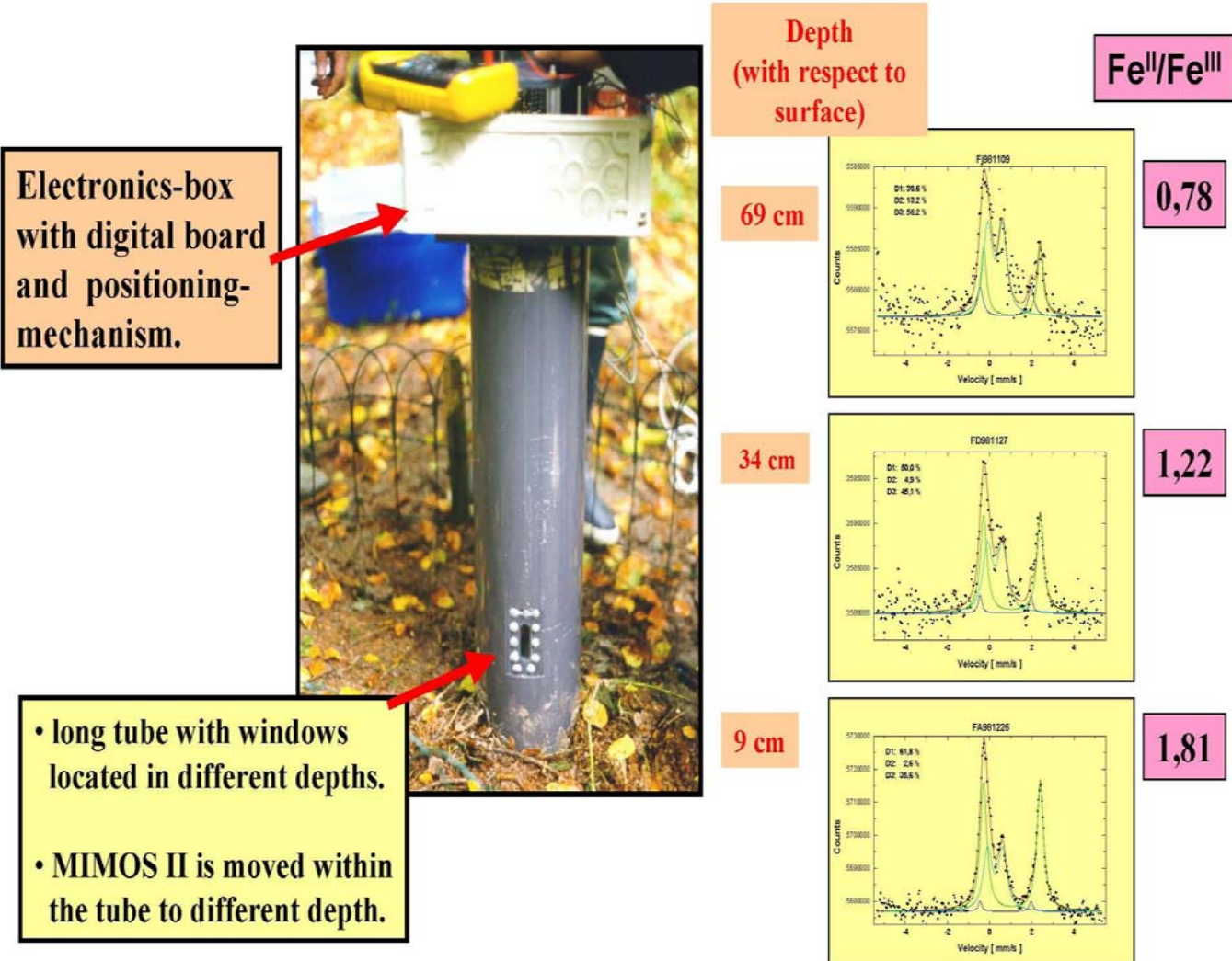
- (1) the **mineralogical identification** of iron-bearing phases (e.g., oxides, silicates, sulfides, sulfates, and carbonates),
- (2) the **quantitative measurement of the distribution of iron** among these iron-bearing phases (e.g., the relative proportions of iron in olivine, pyroxenes, ilmenite and magnetite in a basalt), and
- (3) the quantitative measurement of the **distribution of iron among its oxidation states** (e.g., Fe^{2+} , Fe^{3+} , and Fe^{6+}).

First Mössbauer Spectrum Recorded on Martian Surface Gusev Crater, January 17, 2004 (3h25min)



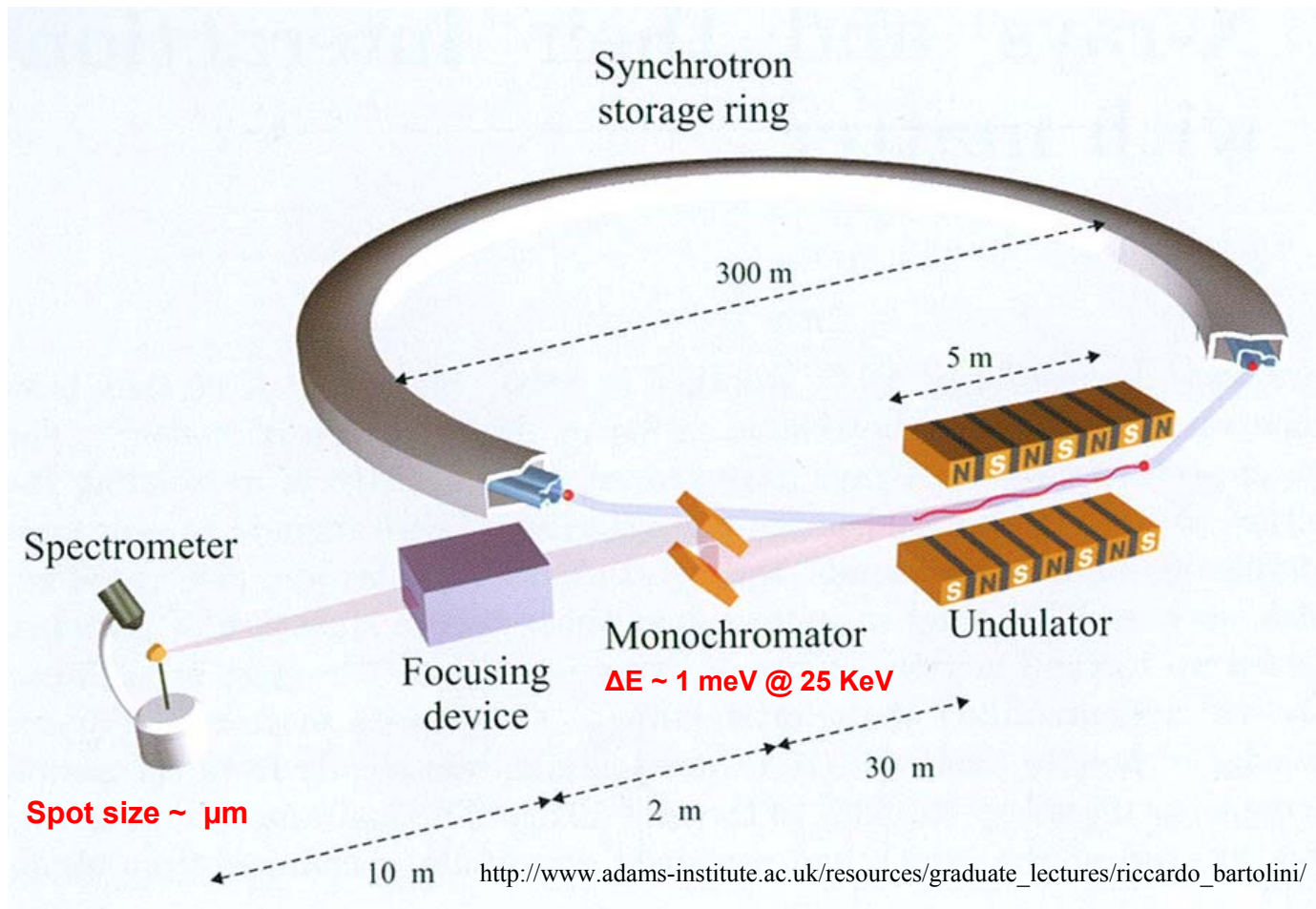
Terrestrial applications of MIMOS II

Monitoring of Iron Mineralogy and Oxidation States in the Field: the Green Rust Mineral



SR-based Mössbauer spectroscopy

SR: Synchrotron radiation: The electromagnetic radiation emitted when charged particles are accelerated radially. It is produced in the synchrotron radiation sources using **bending magnets, undulators and wigglers**



Properties of synchrotron radiation

Broad Spectrum from microwaves to hard X-rays:
the users can select the wavelength required for their experiment.

Monochromators $\Delta E \geq 1 \text{ meV @ } 25 \text{ KeV}$

High Brilliance:

highly collimated photon beam generated by a small divergence and small size source (spatial coherence)

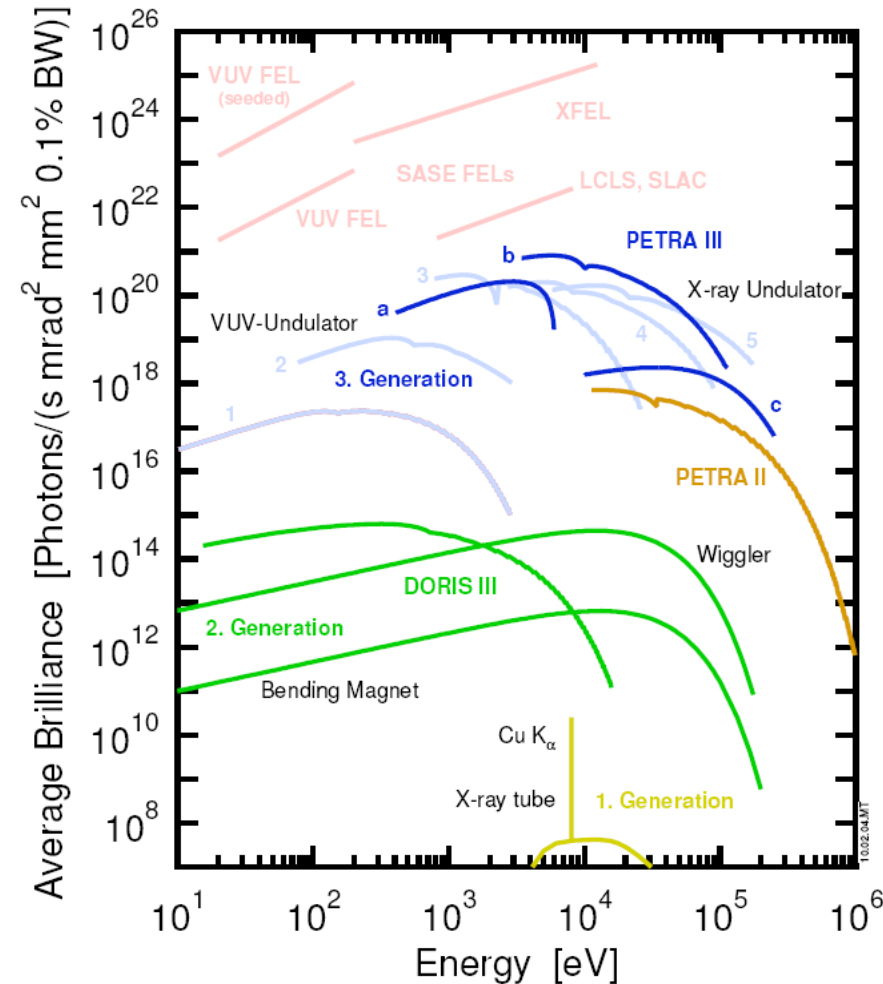
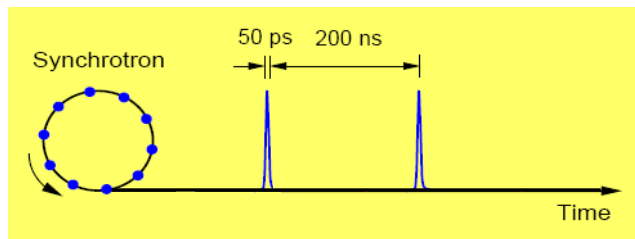
Focussing of hard X-rays down to a spot size of $< 100 \text{ nm}$ has been demonstrated at ESRF

High Stability: submicron source stability

Polarization: both linear and circular

Pulsed Time Structure:

pulsed length down to tens of picoseconds
Pulse separation: 2 ns to 4 μs



2005: Worldwide about 40.000 scientists are using synchrotron radiation

SR Mössbauer spectroscopy – Nuclear resonant scattering

Conventional Mössbauer spectroscopy with radioactive sources is difficult when narrow , high intensity beams of γ -rays are needed for e.g. the study of **very small samples, ultrathin films samples and, under high pressures**

Synchrotron radiation is a very powerful instruments for such studies because of its properties: **Tunable energy, high brilliance, small beam size, small beam divergence and pulsed time structure.**

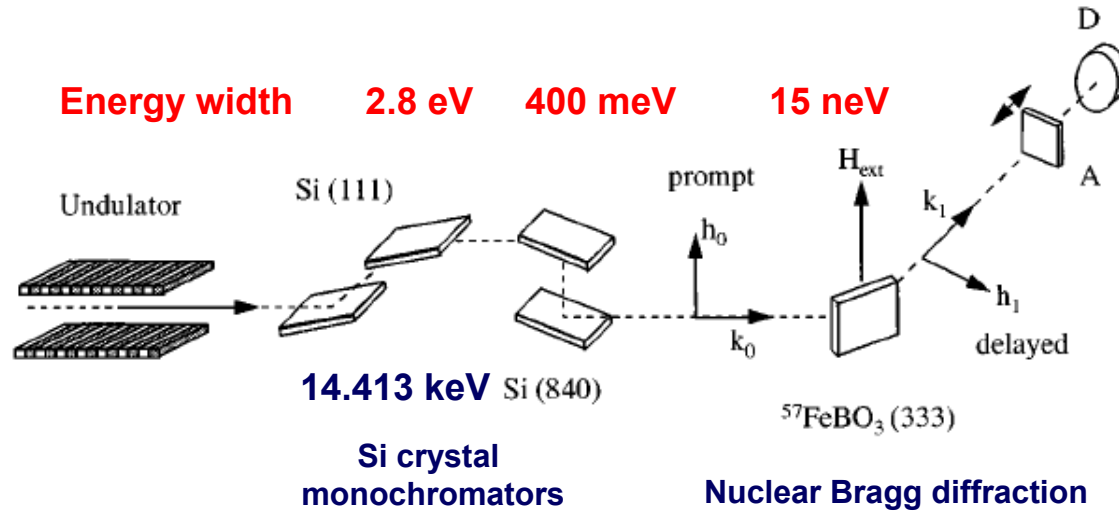
SR Mössbauer studies can be carried out in

- (i) the energy domain:**
observation of the nuclear resonant scattering as a function of energy
- (ii) The time domain:**
Time differential observation of the scattered intensity

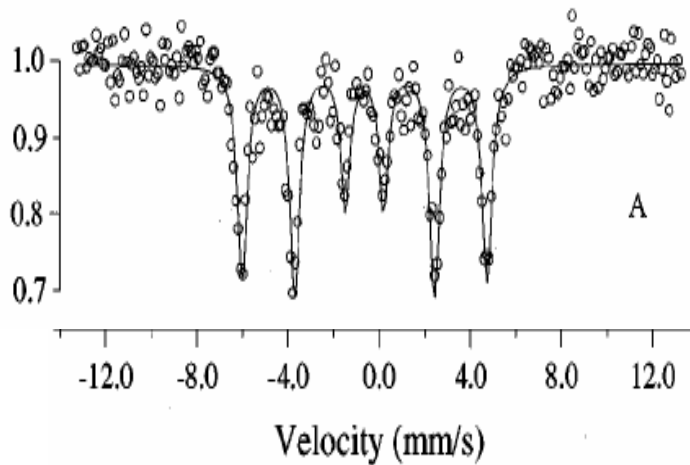
Presently, most of the nuclear resonant scattering studies are carried out in the time domain

SR Mössbauer spectroscopy in the energy domain

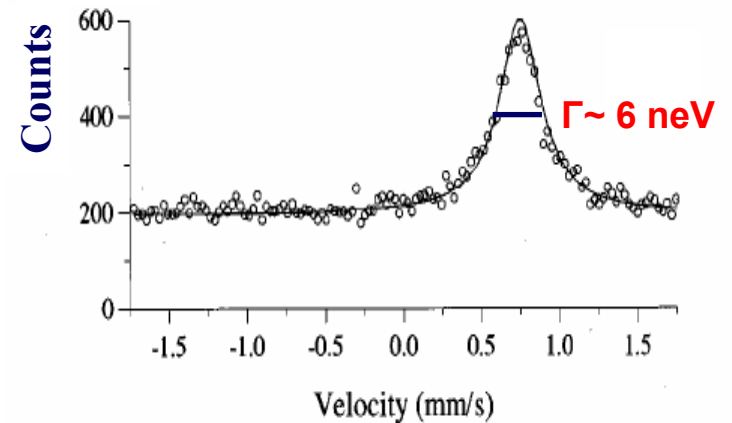
A ^{57}Fe Synchrotron Mössbauer Source G. V. Smirnov et al. PRB 55 (1997) 5811



Absorber ^{57}Fe foil



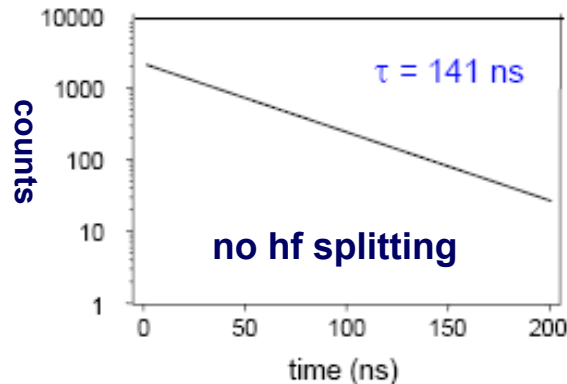
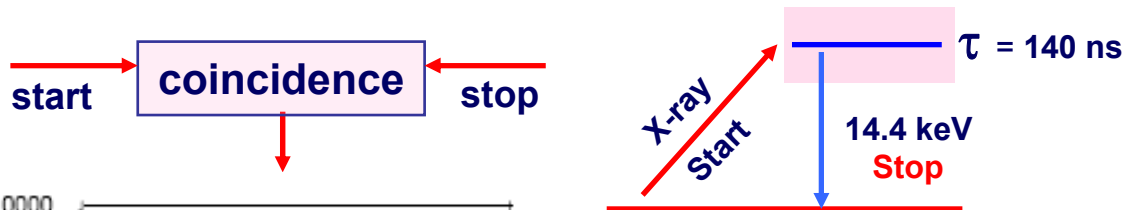
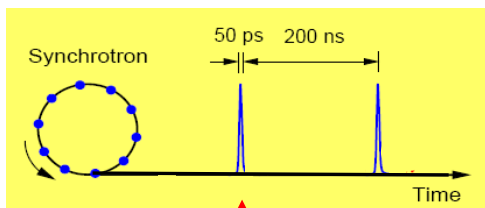
absorber of sodium nitroprusside



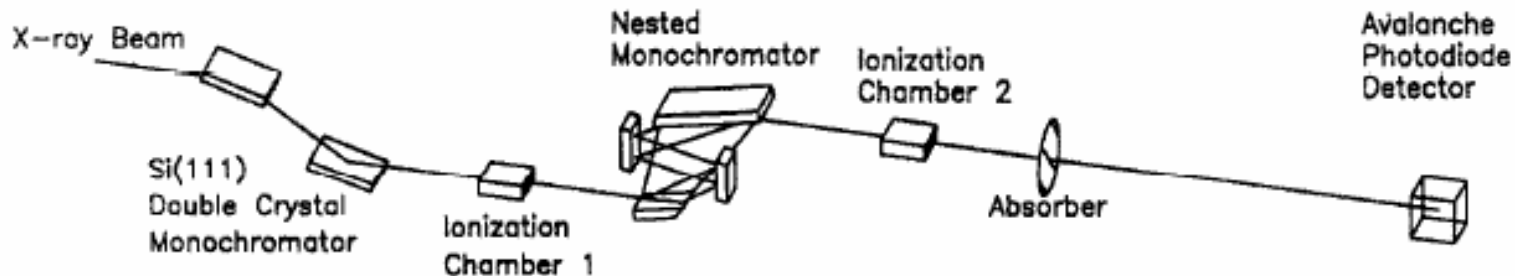
SR Mössbauer spectroscopy in the time domain

Time differential observation of nuclear resonance scattering

SR time structure

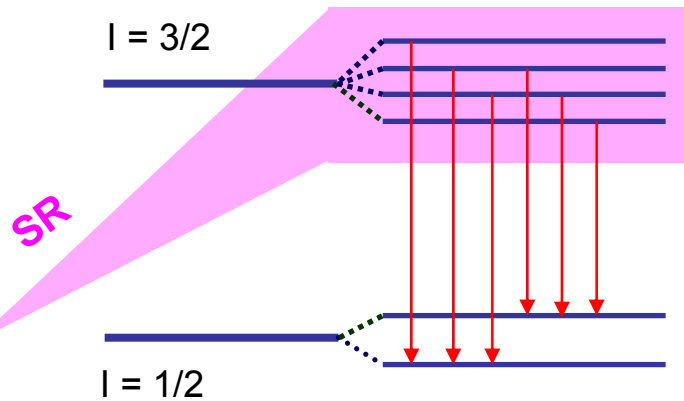


E.E. Alp et al.,
Nucl. Instr. Methods B 97 (1995) 526-529



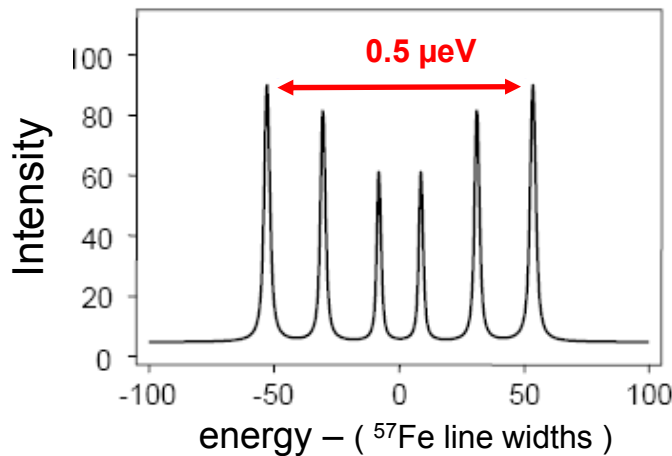
SR Mössbauer spectroscopy in the time domain

Time spectra in the presence of hyperfine interactions

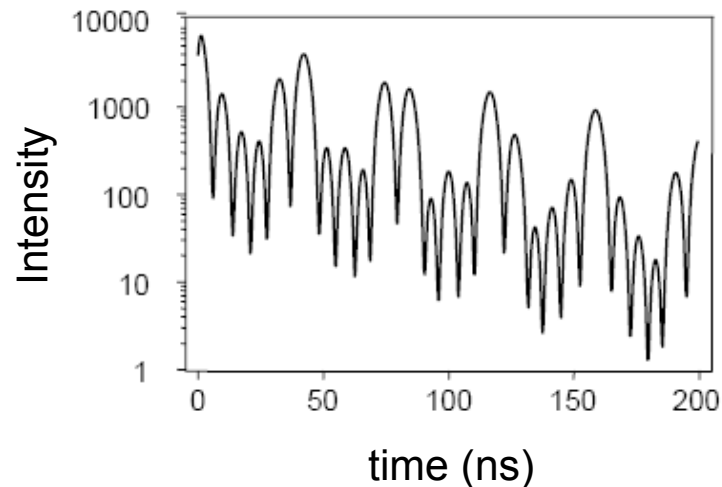


Simultaneous broad band excitation of all hyperfine levels results in **interference** between the different nuclear transitions and fast **quantum beats** in the time spectrum

Corresponding energy spectrum

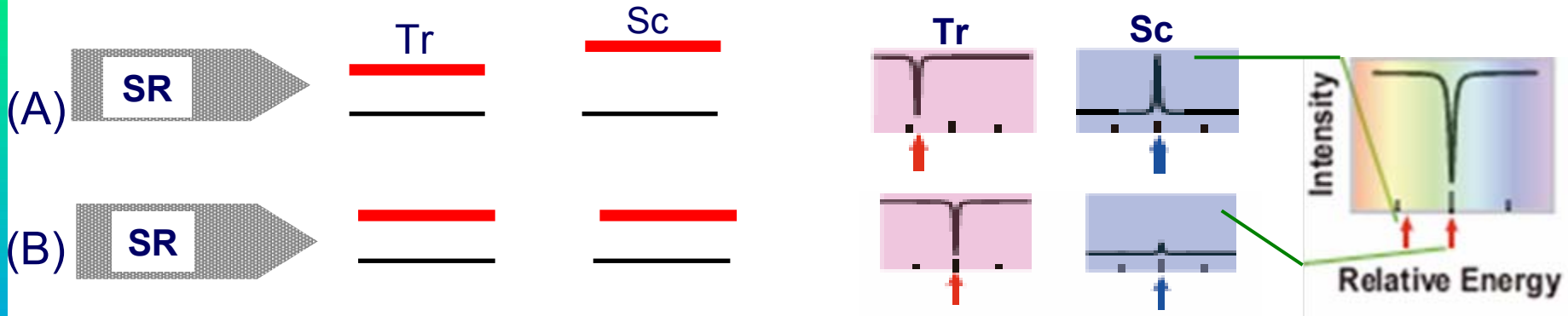
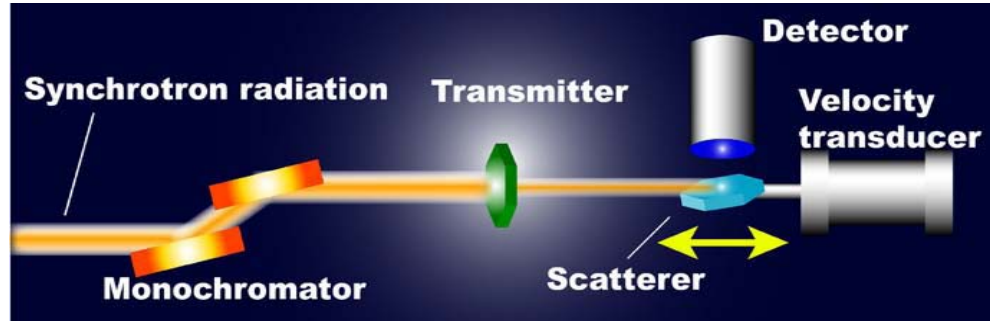


Time spectrum



SR Mössbauer spectroscopy in the energy domain

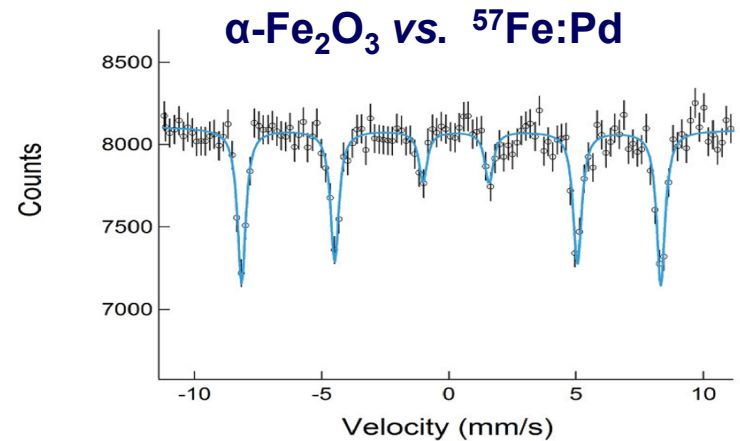
M. Seto et al.
 PRL 102, 217602 (2009)
 Journal of Physics: Conference
 Series 217 (2010) 012002



(A): Different resonance energies of transmitter $E_0(\text{Tr})$ and scatterer $E_0(\text{Sc})$, high transmission at the resonance $E_0(\text{Sc})$, strong scattered intensity at $E_0(\text{Sc})$

(B): Equal resonance energies $E_0(\text{Tr})$ and $E_0(\text{Sc})$. Weak transmission and minimum of the scattered intensity

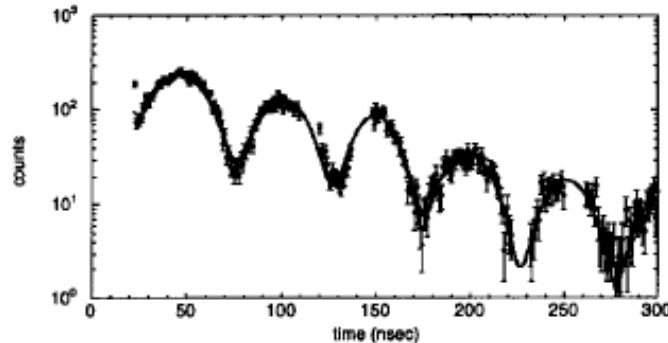
The hyperfine pattern can therefore be sampled by relative motion of scatterer and transmitter



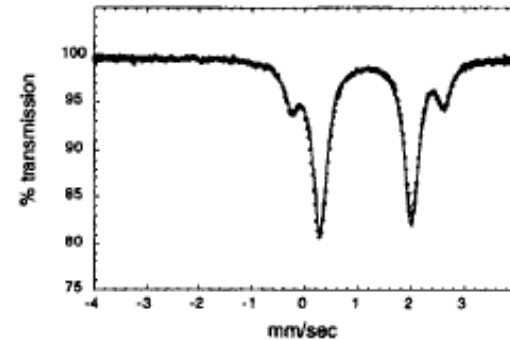
Comparison of Mössbauer spectra in the time- and the energy domain

Example: $\text{Fe}(\text{NH}_4)_2(\text{SO}_4)_2 \cdot 6\text{H}_2\text{O}$

Time domain
using Synchrotron radiation



Energy domain
Transmission spectrum
using a radioactive source



Comparison of results obtained by synchrotron Mossbauer spectroscopy, SMS, and transmission Mossbauer spectroscopy experiments

E.E. Alp et al.,
Nucl. Instr. Methods
B 97 (1995) 526-529

Parameter	SMS	Transmission Mossbauer
<i>Component 1</i>		
Isomer shift [mm/s]	1.41 ± 0.02	1.36 ± 0.02
Quadrupole splitting [mm/s]	1.71 ± 0.008	1.73 ± 0.02
Relative weight	0.79 ± 0.06	0.88 ± 0.001
<i>Component 2</i>		
Isomer shift [mm/s]	1.41 ± 0.24	1.41 ± 0.02
Quadrupole splitting [mm/s]	2.83 ± 0.43	2.82 ± 0.02
Relative weight	0.21 ± 0.13	0.15 ± 0.003